Experimental and modeling investigation of the effect of the unsaturation degree on the gas-phase oxidation of fatty acid methyl esters found in biodiesel fuels

Anne Rodriguez, Olivier Herbinet, Frédérique Battin-Leclerc, Alessio Frassoldati, Tiziano Faravelli, Eliseo Ranzi

Experimental and modeling investigation of the effect of the unsaturation degree on the gas-phase oxidation of fatty acid methyl esters found in biodiesel fuels

Anne Rodriguez[1], Olivier Herbinet[1], Frédérique Battin-Leclerc[1],
Alessio Frassoldati[2], Tiziano Faravelli[2], Eliseo Ranzi[2]

[1] *Laboratoire Réactions et Génie des Procédés, UMR 7274 CNRS – Université de Lorraine, 1 rue Grandville, 54000 Nancy, France*
[2] *Dipartimento di Chimica, Materiali e Ingegneria Chimica "G. Natta" Politecnico di Milano, Piazza Leonardo da Vinci 32, 20133 Milano, Italy*

*Corresponding author information:

For questions about experiments:

Olivier HERBINET
Laboratoire Réactions et Génie des Procédés
Ecole Nationale Supérieure des Industries Chimiques
BP 20451
1 rue Grandville
54000 Nancy, France
Tel: +33 (0)3 83 17 53 60
Fax: +33 (0)3 83 17 81 20
E-mail: olivier.herbinet@univ-lorraine.fr

For questions about modeling:

Eliseo Ranzi
Department of Chemistry, Materials and Chemical Engineering
Politecnico di Milano
Piazza Leonardo da Vinci, 32
20133 Milano, Italy
Tel: +390223993250
Fax: +390270638173
E-mail: eliseo.ranzi@polimi.it

Experimental and modeling investigation of the effect of the unsaturation degree on the gas-phase oxidation of fatty acid methyl esters found in biodiesel fuels

Anne Rodriguez[1], Olivier Herbinet[1], Frédérique Battin-Leclerc[1],
Alessio Frassoldati[2], Tiziano Faravelli[2], Eliseo Ranzi[2]

[1] *Laboratoire Réactions et Génie des Procédés, UMR 7274 CNRS – Université de Lorraine, 1 rue Grandville, 54000 Nancy, France*
[2] *Dipartimento di Chimica, Materiali e Ingegneria Chimica "G. Natta" Politecnico di Milano, Piazza Leonardo da Vinci 32, 20133 Milano, Italy*

Abstract

The oxidation of three C_{19} fatty acid methyl esters present in biodiesel fuel was experimentally investigated using a jet-stirred reactor in order to highlight the effect of double bonds on the reactivity and product distribution. Fuel candidates were methyl-stearate, methyl oleate and methyl linoleate with no, one and two double bonds, respectively. Experiments were carried out over a wide temperature range (500–1050 K), at a pressure of 1.067 bar, at a residence time of 2 s. Methyl esters were diluted with benzene to avoid their condensation as much as possible. Inlet mole fractions of methyl ester, benzene and oxygen were 4×10^{-4}, 5×10^{-3} and 4.5×10^{-2}, respectively (with dilution in helium). However, as previously demonstrated for alkanes, the presence of benzene does not notably influence the mixture reactivity below 850 K. Many reaction intermediate products have been quantified, including species which can be formed through Waddington reaction for unsaturated reactants. The present experiments are the first ones allowing the actual measurement of large ester intrinsic reactivity in a jet-stirred reactor. They further contribute to an extensive validation of the POLIMI lumped kinetic scheme of pyrolysis and oxidation of biodiesel fuels. Two reaction classes have been added to better account for the oxidation of species with double bonds: the Waddington mechanism and the concerted decomposition reactions through cyclic transition states. The new model contains 18,217 reactions involving 461 species. Overall, a correct agreement was obtained for the reactivity of the three fuels. The model well reproduces mole fraction profiles of many reaction products. The kinetic analysis performed at low-temperature (650 K) confirmed the significant inhibitive effect of H-atom abstractions forming non-propagating allyl type radicals in this temperature region. It also showed that the inhibitive effect of these reactions increases from methyl oleate to methyl linoleate, which explains the large difference observed in the reactivity.

Keywords

Biodiesel; Fatty acid methyl-esters; Jet-stirred reactor; Low temperature combustion; Detailed kinetic of oxidation

1. Introduction

The continuously increasing world energy demand and the negative impact of the use of fossil fuels on the environment have led to a shift toward alternative sources of energy such as biofuels. Without waiting for new technologies, the depletion of oil resources and the preservation of the environment urge us to improve as much as possible the current engines fed with biofuels. Biodiesel, which is a blend of fatty acid methyl esters obtained from the trans-esterification of vegetable oil or animal fat, is one of the transportation fuels which are currently used in diesel engines [1]. This alternative fuel has several advantages compared to petroleum fuels: it is a renewable energy source which can be blended with other resources like diesel fuel. It is sulfur free and it has interesting lubricating properties [2]. Biodiesel has also some disadvantages due to some of its physical properties (e.g., higher viscosity which affects the operation of injectors, the presence of unsaturations which makes biodiesel less stable and requires the addition of stabilizers for the storage) [3]. As far as emissions are concerned, the use of biodiesel instead of diesel fuel in a diesel engine leads to a decrease of particulate matter, unburned hydrocarbons, sulfur oxides, carbon monoxide and volatile organic compounds, but leads to an increase of nitrogen oxides [4].

The composition of fatty acid methyl esters found in biodiesel fuels depends on the plant it is issued [4] (Table 1). As an example, rapeseed oil methyl ester is composed of 62% of methyl oleate ($C_{19}H_{36}O_2$). It also contains methyl linoleate ($C_{19}H_{34}O_2$), methyl linolenate ($C_{19}H_{32}O_2$), methyl stearate ($C_{19}H_{38}O_2$) and methyl palmitate ($C_{17}H_{34}O_2$). Soybean oil methyl ester also contains the same species but with a different composition: methyl palmitate and methyl oleate are the main components.

Table 1: Average composition (wt%) of some biodiesel fuels issued from plants [4].

	methyl palmitate $C_{17}H_{34}O_2$	**methyl stearate $C_{19}H_{38}O_2$**	**methyl oleate $C_{19}H_{36}O_2$**	**methyl linoleate $C_{19}H_{34}O_2$**	**methyl linolenate $C_{19}H_{32}O_2$**
rapeseed oil methyl esters	4	2	62	22	10
soybean oil methyl esters	12	4	23	54	6
palm oil methyl esters	43	4	41	10	0

These esters have very close structures (Table 2): they are composed of a long alkyl chain (16–18 carbon atoms) attached to a methyl ester group. The difference is the number of double bonds in the chain (no, 1, 2 or 3 double bonds). As for alkenes, the degree of unsaturation (i.e., the number of double bonds) has a direct influence on the low-temperature oxidation chemistry and reactivity of methyl esters. This is responsible for the large difference which is observed in the cetane number of these species [5] (Table 2).

The literature is particularly abundant concerning the gas phase oxidation data for small methyl esters [6], [4], [7], [8], [9], [10], [11] and [12]. Methyl butanoate oxidation was extensively studied over a wide range of conditions including flow reactors, jet-stirred reactors, shock tubes, rapid compression machines and flames [4], [6], [9] and [10]. These studies enabled a better understanding of the chemistry specific to this class of biofuels. Nevertheless they also showed that methyl butanoate was not a good surrogate for the large methyl esters actually found in biodiesel fuels.

Table 1: Structure and cetane number of methyl esters [5].

ester	structure	cetane number
methyl palmitate ($C_{17}H_{34}O_2$)	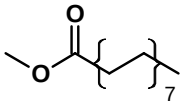	86
methyl stearate ($C_{19}H_{38}O_2$)	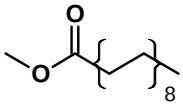	101
methyl oleate ($C_{19}H_{36}O_2$)	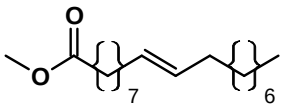	59
methyl linoleate ($C_{19}H_{34}O_2$)	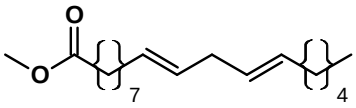	38
methyl linolenate ($C_{19}H_{32}O_2$)	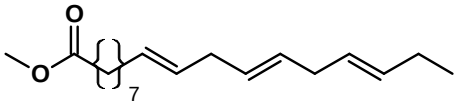	23

Oxidation studies involving saturated esters with an alkyl chain up to C_{10} (e.g., methyl hexanoate, heptanoate, octanoate and decanoate) are also reported in literature [4] and [6]. These studies showed that these species can be good candidates for surrogate of actual saturated methyl esters (e.g., methyl stearate) but not for actual unsaturated methyl esters.

There are only a few data about the gas-phase oxidation chemistry of methyl esters larger than methyl palmitate (Table 3). Fewer data can be found about their low-temperature oxidation chemistry with reaction product analysis. Ignition delay times were measured behind shock waves for methyl palmitate, methyl stearate, methyl oleate and methyl linoleate at high temperatures (above 900 K) [13] and [14]. Campbell et al. [13] compared ignition delay times of methyl oleate and methyl linoleate. This study showed that the two biofuels have about the same reactivity at high-temperatures. In the same way, Wang et al. [14] observed that ignition delay times measured under similar conditions for the four methyl esters were very close and were similar to ignition delay times of real biodiesels (soybean methyl esters and animal fat methyl esters), irrespectively of the presence and number of the double bonds. In contrast, Das et al. [15] observed that sooting tendency of unsaturated methyl esters depends on the number and position of the C=C double bonds. Campbell et al. [16] also succeeded to measure ignition delay times of methyl palmitate which is a waxy solid at room temperature using their aerosol shock tube. Chong et al. [17] measured laminar flame speeds of palm methyl esters (PME) using the jet-wall stagnation flame configuration. They observed that data for PME were very close to laminar flame speeds measured for diesel fuel and blends of PME with diesel. This shows that biodiesel reactivity is similar to that of diesel at high-temperatures. Dagaut et al. [18] studied the oxidation of rapeseed methyl esters (RME) in a jet-stirred reactor at temperatures between 800 and 1400 K (after the negative temperature coefficient zone). They measured mole fractions of small reaction products but no information was reported about species containing ester functions.

Table 2: Summary of experimental data for the oxidation of fatty acid methyl esters and biodiesel fuels.

Species	Reactor[a]	Conditions	Reference
Methyl palmitate	JSR[b]	T = 500 - 1100 K; P = 1 bar; τ = 1.5 s; φ = 1; x_{ester} = 5.2×10^{-4}; $x_{n-decane}$ = 1.48×10^{-3}; in He	[19]
	ST	T = 900 - 1300 K; P = 10 – 20 atm; φ = 0.25 – 1; fuel/air mixture	[14]
	ST	T = 1100 - 1400 K; P = 3.5 – 7 atm; φ = 0.27 – 0.81; x_{O_2} = 0.04 ; in Ar	[16]
Methyl stearate	ST	T = 950 - 1350 K; P = 10 atm; φ = 0.5; fuel/air mixture	[14]
	JSR[c]	T = 500 - 1100 K; P = 1.067 bar; τ = 2 s; $\varphi \approx 1$; x_{ester} = 4×10^{-4}; $x_{benzene}$ = 5×10^{-3}; x_{oxygen} = 0.045; in He	This work
Methyl oleate	JSR[b]	T = 500 - 1100 K; P = 1 bar; τ = 1.5 s; φ = 1; x_{ester} = 5.2×10^{-4}; $x_{n-decane}$ = 1.48×10^{-3}; in He	[20]
	JSR[c]	T = 500 - 1100 K; P = 1.067 bar; τ = 2 s; $\varphi \approx 1$; x_{ester} = 4×10^{-4}; $x_{benzene}$ = 5×10^{-3}; x_{oxygen} = 0.045; in He	This work
	ST	T = 1100 - 1400 K; P = 3.5 – 7 atm; φ = 0.6 – 2.4; x_{ester} = 9×10^{-4} – 3.7×10^{-3}; in Ar	[13]
	ST	T = 950 - 1350 K; P = 10 atm; φ = 0.5; fuel/air mixture	[14]
Methyl linoleate	ST	T = 1100 - 1400 K; P = 3.5 – 7 atm; φ = 0.6 – 2.4; x_{ester} = 9×10^{-4} – 3.7×10^{-3}; in Ar	[13]
	ST	T = 950 - 1350 K; P = 10 atm; φ = 0.5; fuel/air mixture	[14]
	JSR[c]	T = 500 - 1100 K; P = 1.067 bar; τ = 2 s; $\varphi \approx 1$; x_{ester} = 4×10^{-4}; $x_{benzene}$ = 5×10^{-3}; x_{oxygen} = 0.045; in He	This work
PME	Flame[e]	T = 470 K, P = 1 atm; φ = 0.7 – 4.4; fuel air mixture	[17]
RME[d]	JSR	T = 800 - 1400 K; P = 1 - 10 bar; τ = 0.07 – 1 s; φ = 0.25 – 1.5; x_{ester} = 0.0005; in N_2	[18]
SME[d]	ST	T = 950 - 1350 K; P = 10 atm; φ = 0.5; fuel/air mixture	[14]
AFME[d]	ST	T = 950 - 1350 K; P = 10 atm; φ = 0.5; fuel/air mixture	[14]

[a] JSR = jet-stirred reactor; ST = shock tube.
[b] methyl esters blended with *n*-decane.
[c] methyl esters blended with benzene.
[d] PME = palm methyl esters; RME = rapeseed methyl esters; SME = soybean methyl esters; AFME = animal fat methyl esters.
[e] laminar flame speed measurements.

Hakka et al. [19] and Bax et al. [20] have studied the oxidation of methyl palmitate and methyl oleate in a jet-stirred reactor over a wide range of temperatures (500–1100 K). Methyl esters were blended with *n*-decane to decrease the partial pressure of the biofuel and avoid condensation problems between the reactor outlet and gas chromatographs. As explained by Bax et al. [20], the intrinsic reactivity of methyl esters cannot be caught as biofuels were blended with n-decane which exhibited a high reactivity even at low-temperatures. The alkane presence enhances the reactivity of esters thanks to reactions of the radical pool. Many reaction products were measured during these two studies. As an example, 10 unsaturated esters (from methyl acrylate to 14-pentadecene methyl ester) produced by β-scission decomposition reactions were observed in the oxidation of methyl palmitate. In the same way, the formation of many cyclic ethers (with a tetrahydrofuran cycle and an ester function) were also detected [19]. Reaction products typically observed during the oxidation of alkenes [21] were also detected during the oxidation of methyl oleate [20]. For example the oxirane compound which is obtained by the addition of an HO_2 radical on the double bond and ketones formed through the Waddington mechanism were detected.

As far as modeling studies are concerned, many models for the oxidation of methyl butanoate have been proposed (see [4] for a review of these models). Several of these studies confirmed that methyl butanoate was not a good surrogate for methyl esters actually included in biodiesel since the length of the chain was too short to well predict the reactivity of these species at low-temperature. The size of the models for large methyl esters is larger than that of alkanes with the same of number of atoms of carbon in the molecule because of the absence of symmetry. In line with the development of EXGAS for large alkanes [22], Herbinet et al. developed detailed kinetic models for the oxidation of saturated esters using this software the automatic generation of mechanisms [23]. They proposed a model for the oxidation of methyl palmitate containing more than 4400 species and 30,400 reactions. This model was tested against JSR experimental data [19]. These studies showed that large methyl esters have about the same reactivity over the low- and high-temperature regions. Westbrook et al. developed a detailed kinetic model containing the oxidation chemistry of the five main methyl esters found in rapeseed and soybean biodiesel fuels (this model contains more than 4800 species involved in about 20,000 reactions) [5] and [24]. These models were tested against the very few available JSR experimental data from the literature [18], [19] and [20]. More recently, based on the long used POLIMI modeling approach [25], Saggese et al. used a lumped approach for the kinetic modeling of the pyrolysis and combustion of biodiesel [26] taking advantage from the work of Westbrook et al. [5]. The obtained model contained about only 420 species and 13,000 reactions making it a more flexible tool for modeling applications.

The first goal of this paper is to provide new quantitative experimental data for the oxidation of methyl esters present in biodiesel fuels over a wide range of temperatures (from 500 to 1050 K covering both the low- and high-temperature oxidation zones), with a particular focus on the effect of unsaturations in the alkyl side chain on the intrinsic reactivity. Species investigated are the three methyl esters with a C_{18} alkyl chain: methyl stearate, methyl oleate and methyl linoleate, with no, one and two double bonds, respectively. As these species are poorly volatile due to their high molecular weight and the presence of oxygen atoms, they were diluted in benzene to avoid condensation. During a previous oxidation study of a *n*-decane/benzene blend [27], it was shown that benzene had almost no reactivity and had then negligible influence on alkane reactivity at low-temperatures (below 800 K).

Based on these new experimental results, the second objective of this paper is to present the recent improvements in the POLIMI lumped kinetic scheme of pyrolysis and oxidation of biodiesel fuels [26]. New types of reactions have been added to better account for the specific oxidation chemistry which occurs due to the presence of the double bond: the Waddington mechanism [28] and [29] (leading to the formation of aldehydes starting from the addition of OH radicals to the double bond) and decomposition of unsaturated species through concerted mechanism involving cyclic transitions states. The kinetic model is then compared to JSR data obtained in the present study as well as data from the literature. A kinetic analysis was performed in order to explain the large difference of reactivity between the different fuels in the low-temperature region.

2. Experimental apparatus

The oxidation of methyl esters was performed using a fused silica jet-stirred reactor. This reactor is a type of continuous stirred tank reactor operated at steady state. It is well adapted to kinetic studies since operating conditions are well defined (constant temperature, pressure, residence time and gas mixture inlet composition). Its behavior is represented by very simple equations derived from mass and energy balances enabling easy simulations with detailed kinetic models. This reactor has already been used to study several gas-phase oxidation and pyrolysis studies [30]. Experiments were performed at temperatures in the range 500–1100 K, a pressure of 1.067 bar and a residence time of 2 s. Inlet mole

fractions in the investigated gas mixture were $4 \times 10^{-4}/5 \times 10^{-3}/0.045/0.95$ for methyl ester, benzene, oxygen and helium, respectively. The ester mole fraction was chosen to have a boiling point in the range 403.15–413.15 K, well below the temperature of the evaporator (473.15 K). The relation between the ester partial pressure and the boiling point was obtained with Antoine equation parameters available from the NIST WebBook [31].

Mass flow controllers were used to feed the reactor with oxygen and helium. Accuracy given by the manufacturer (Bronkhorst) is 0.5%. A Coriolis flow controller was used for the feed of the liquid fuel mixture (mixture of methyl ester and benzene). The accuracy indicated by the manufacturer is 0.5%. The liquid fuel mixture was mixed with helium and evaporated in a heat exchanger also provided by Bronkhorst (with the temperature set at 473.15 K, well above the boiling point of ester fuels under the conditions of this study). Uncertainties in reactant flows have very small effects on residence time which was 2.00 ± 0.01 s.

The reactor and preheating zone were heated with Thermocoax heating wires rolled around the different parts and the temperature was controlled using type K thermocouples. It was shown that the preheating was of great importance to obtain the temperature homogeneity of the gas phase in the jet-stirred reactor [32]. The temperature homogeneity is also favored by the high dilution in helium. The reaction temperature was measured using an independent type K thermocouple located in a glass finger inside the reactor. The uncertainty in temperature measurement was estimated to ± 2 K.

The pressure was controlled using a valve located downstream of the reactor outlet. The pressure was read with a MKS pressure transducer. The uncertainty was ± 0.01 bar. Working at a pressure above the atmospheric one was necessary to push the flow towards gas chromatograph valves.

Analyses were performed using gas chromatography. Two methods were used for the sampling. For low molecular weight species (permanent gases and organic compounds with less than five carbon and oxygen atoms), analyses were performed online by injecting the loop content of a gas sampling valve swept by the gas flow from the reactor outlet through a transfer line heated up to 453 K. The loop was in a valve box heated up to 473.15 K to avoid condensation. For species with higher molecular weights (e.g., methyl ester fuel) the sampling was performed by collecting species in a trap located at the reactor outlet and maintained at liquid nitrogen temperature. The content of the trap was then injected into a gas chromatograph with an automatic sampler after warming up to the ambient temperature and addition of solvent (acetone, with a short residence time when using an HP-5 capillary column) and a known amount of internal standard (*n*-octane).

Two gas chromatographs were used for the quantification of low molecular weight species. One was equipped with a Carbosphere packed column and a thermal conductivity detector for the quantification of oxygen. The other was equipped with a Plot Q capillary column and a flame ionization detector for the detection of carbon containing species. A methanizer (nickel catalyst for hydrogenation) located between the column outlet and the detector was used to make possible the detection of $C_1H_xO_y$ species like CO, CO_2 and formaldehyde. In both apparatuses the temperature of the injector was set at 523.15 K.

A gas chromatograph equipped with a HP-5 capillary column and a flame ionization detector was used for the offline analysis of higher molecular weight species. A similar apparatus equipped with an impact electronic mass spectrometer operated under the same conditions was used for the identification of reaction products.

The detection limit was about 1 ppm for species quantified using a flame ionization detector. The relative uncertainty in mole fractions was estimated to ± 5% for species calibrated using standards and whose peaks are not co-eluted. It is ± 10% for species calibrated using the effective carbon number method and species whose peak is co-eluted. The effective carbon number method relies on the sensitivity of this detector to the number of carbon atoms present in the species [33] and [34] (e.g., it is assumed that 2-butene isomers and *iso*-butene have the same response as 1-butene with a flame ionization detector, or that n-butane as response which is twice that of ethane).

3. Experimental results

Under the conditions previously described, mole fraction profiles of reactants are displayed in Figure 1. Significant differences can be spotted in the mole fraction profiles of the three methyl esters, especially at low-temperature (below 750 K). As expected, methyl stearate is the most reactive species with a conversion of 75% at 650 K, and a marked negative temperature coefficient behavior from 650 to 750 K. The least reactive fuel is methyl linoleate with a very narrow zone of reactivity between 625 and 725 K and a maximum conversion of about 20%. Methyl oleate is laying in between the two other ester fuels with a maximum conversion of about 54% at 650 K. While the reactivity is going down to zero at the end of the negative temperature coefficient (NTC) region for the two unsaturated methyl esters, methyl stearate still exhibits reactivity in this region with a minimum conversion of 30% at 750 K. Contrary to ester fuels, only slight differences are observed in the mole fraction profiles of benzene and oxygen. For O_2 (Figure 1), the main differences are visible in the temperature range following the NTC region (750–900 K) where mole fractions are larger for methyl oleate than for the two other esters. This is in agreement with the reactivity order of the three esters fuels in this temperature range. For benzene, a slight consumption is observed at low-temperature in the range 600–700 K. This consumption is induced by the high reactivity of methyl stearate visible in Figure 1 and is confirmed by the formation of phenol. Differences are also visible above 900 K. Mole fractions of benzene are lower for methyl linolenate than for the two other fuels. This is in agreement with the higher reactivity of methyl linolenate in this temperature range. Nevertheless these observations should be regarded with hindsight because of the experimental uncertainties in mole fractions (relative uncertainty of ±10%).

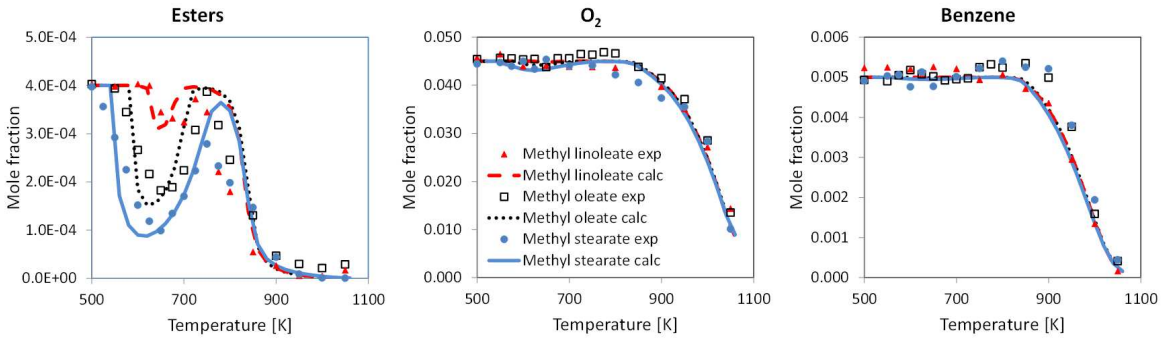

Figure 1: Mole fraction profiles of reactants (P = 106.7 kPa, τ = 2 s, x_{ester} = 4×10^{-4}, $x_{benzene}$ = 5×10^{-3}, x_{O_2} = 0.045). Symbols are for experiments and lines for simulations.

Figures 2 and 3 display mole fraction profiles of a selection of reaction products (the whole set of experimental mole fractions is given as Supplementary material). Species which were identified during the experiments with the three esters fuels are mainly low molecular weight species (Figure 2):

- CO, CO_2, CH_2O, CH_3OH, oxirane, CH_3CHO, ethylene oxide,
- CH_4 and all C_2H_x and C_3H_y hydrocarbons.

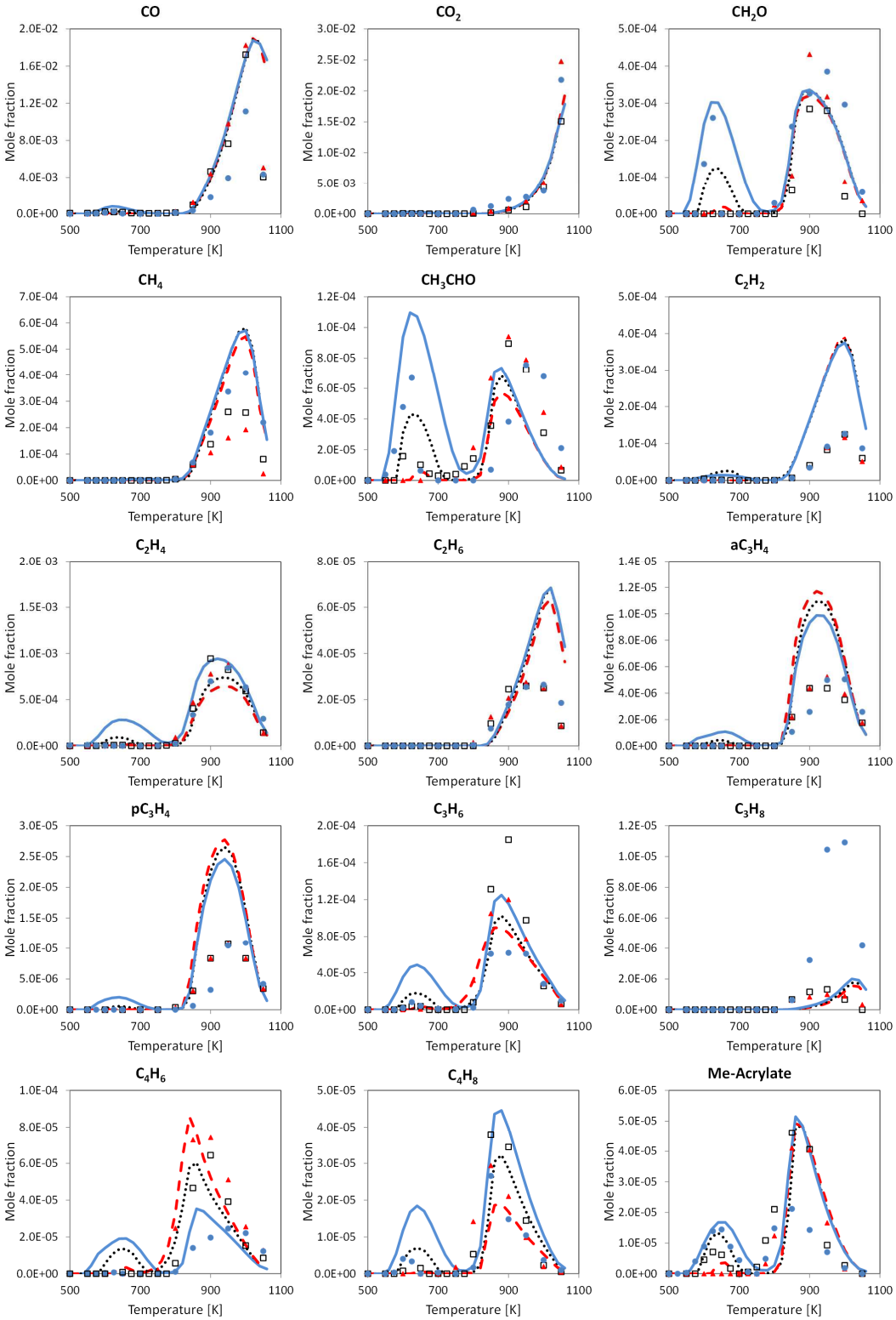

Figure 2: Mole fraction profiles of C_1-C_4 reaction products (P = 106.7 kPa, τ = 2 s, x_{ester} = 4×10^{-4}, $x_{benzene}$ = 5×10^{-3}, x_{O_2} = 0.045). Symbols are for experiments and lines for simulations.

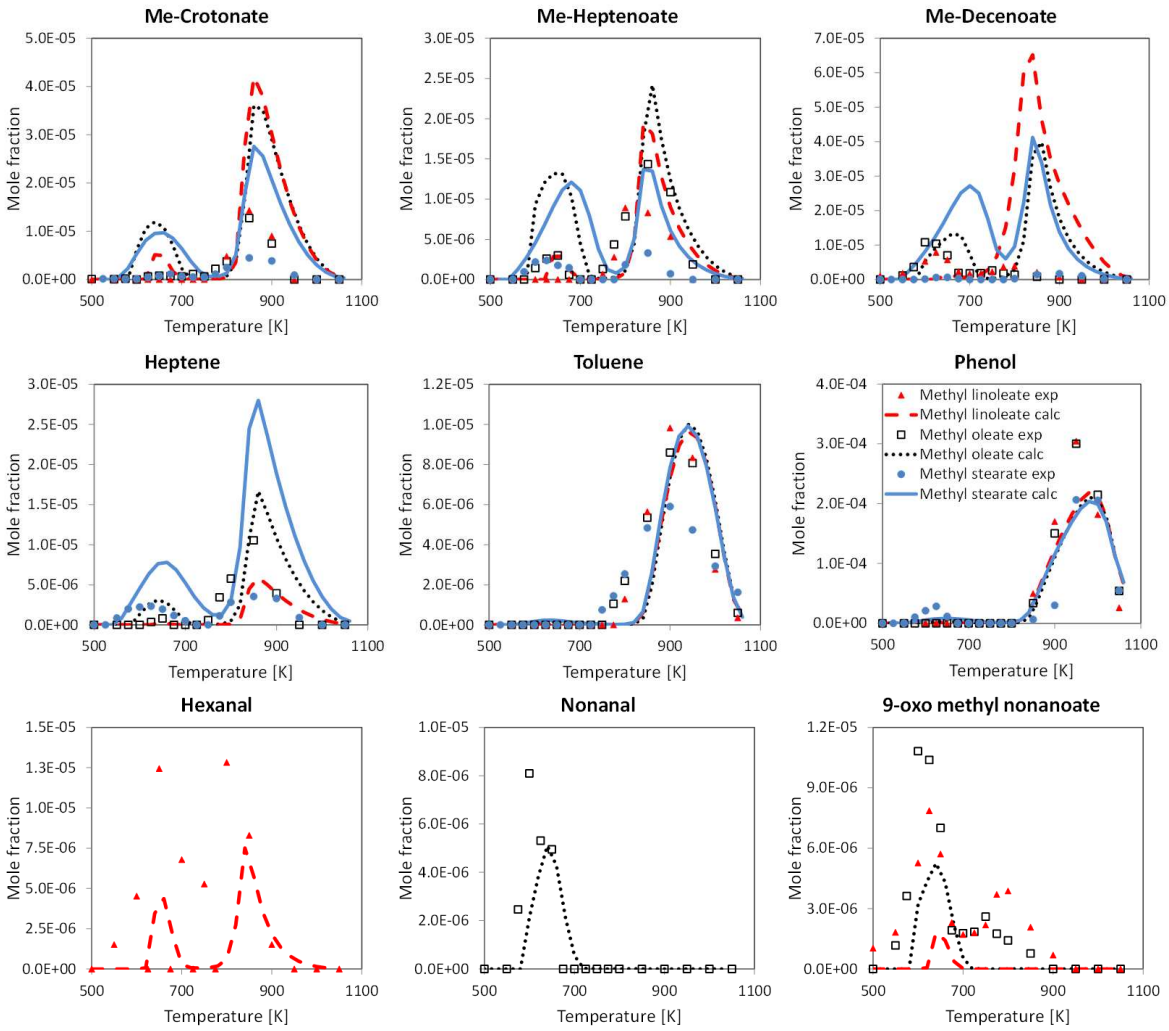

Figure 3: Mole fraction profiles of C_{5+} reaction products (P = 106.7 kPa, τ = 2 s, x_{ester} = 4×10^{-4}, $x_{benzene}$ = 5×10^{-3}, x_{O_2} = 0.045). Hexanal (due to the lumping strategy, the simulated species is hexenal), nonanal and 9-oxo methyl nonanoate are Waddington reaction products. Symbols are for experiments and lines for simulations.

Larger species detected during this study have more specific structures due to the presence or not of double bonds in initial fuels. These species are listed in Table 4.

Table 3: List of reaction products (with at least four carbon atoms) detected in the present study. MS, MO and ML are for methyl stearate, methyl oleate and methyl linoleate, respectively. The "X" symbol indicates that the species was detected during the oxidation of the fuel.

Name	Formula	Structure	MS	MO	ML
Unsaturated hydrocarbons					
1-butene	C_4H_8	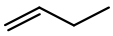	X	X	X
1,3-butadiene	C_4H_6	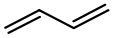	X	X	X
1-pentene	C_5H_{10}		X	X	
1-hexene	C_6H_{12}		X	X	
1-heptene	C_7H_{14}		X	X	
1-olefins from 1-octene to 1-hexadecene	$C_8H_{16} \rightarrow C_{16}H_{32}$	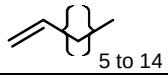	X		
Unsaturated esters					
Methyl acrylate	$C_4H_6O_2$	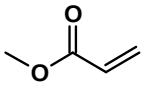	X	X	X
Methyl crotonate	$C_5H_8O_2$	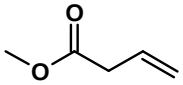	X	X	X
Methyl 6-heptenoate	$C_8H_{14}O_2$	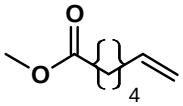	X	X	X
Methyl 7-octenoate	$C_9H_{16}O_2$	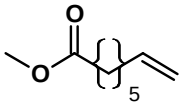	X	X	
From Methyl 8-nonenoate to Methyl 16-heptadecenoate	$C_{10}H_{18}O_2 \rightarrow C_{18}H_{34}O_2$	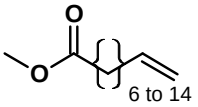	X		
Methyl dodeca-9,11-dienoate	$C_{13}H_{22}O_2$	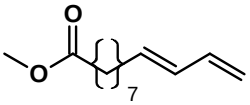		X	
Species with an aldehyde function					
hexanal	$C_6H_{12}O$	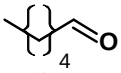			X
nonanal	$C_9H_{18}O$	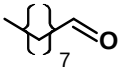		X	
9-oxo,methyl nonanoate	$C_{10}H_{18}O_3$	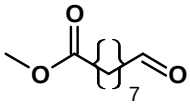		X	X

3.1. Specific species observed in the oxidation of methyl stearate

For methyl stearate, many 1-olefins and methyl esters with one terminal double bond were observed. These types of species have been observed previously [19]. 1-Nonene is missing in the list of detected 1-olefins likely because of a low mole fraction and co-elution. Five membered ring cyclic ethers detected in [19] could not been quantified during the present study due to a lower fuel inlet mole fractions.

3.2. Specific species observed in the oxidation of methyl oleate

For methyl oleate, several olefins and methyl esters with one double bond at the extremity of the chain were also observed, but the variety of these types of species is more limited because of the presence of the double bond in the middle of the chain. As an example, the largest 1-olefin detected in methyl oleate oxidation is 1-heptene (see Table 4) and the largest mono-unsaturated methyl ester is the methyl 6-heptenoate (see Table 4 for the structure of this species). A larger species, but with two double bonds, has been spotted: this is the methyl dodeca-9,11-dienoate (its structure is given in Table 4). The formation of other methyl esters with two double bonds and diolefins was expected but these species were not detected due to a too low fuel inlet mole fraction. Another type of species, usually observed in olefin oxidation chemistry, was identified. These species are aldehydes obtained through the Waddington mechanism: 9-oxo,methyl nonanoate (its structure is shown in Table 4) and nonanal (see Figure 3 for mole fraction profiles of these species). The Waddington mechanism is further discussed in Section 4.1 . The oxirane species which could be obtained from the addition of HO_2 radicals on the fuel double bond was not observed in the present study. In the same way, unsaturated ketones which could be obtained from the combination of allylic fuel radicals and HO_2 radicals could not be detected (whereas this type of species is usually observed in the oxidation of olefins [21] and [35]).

3.3. Specific species observed in the oxidation of methyl linoleate

For methyl linoleate, which has two double bonds, the largest olefin detected is 1-butene. This is fully consistent with the position of the double bond which is located towards the end of the alkyl chain. In the same way, the largest methyl ester identified in methyl linoleate oxidation in this work having one double bond at the end of the chain is methyl 6-heptenoate, such as for methyl oleate. This is because the first double bond is at the same location in both fuels. Species with two double bonds or more have not been detected. As far as species formed from the Waddington mechanism are concerned, amongst the expected products shown in Figure 4, Table 4 shows that only hexanal and 9-oxo,methyl nonanoate were detected (see Figure 3 for mole fraction profiles of these species). The formation of 3-nonenal and 12-oxo,methyl dodeca-9-enoate was expected, but these species were not seen due to the high dilution and the very low-reactivity of this fuel in the low-temperature region.

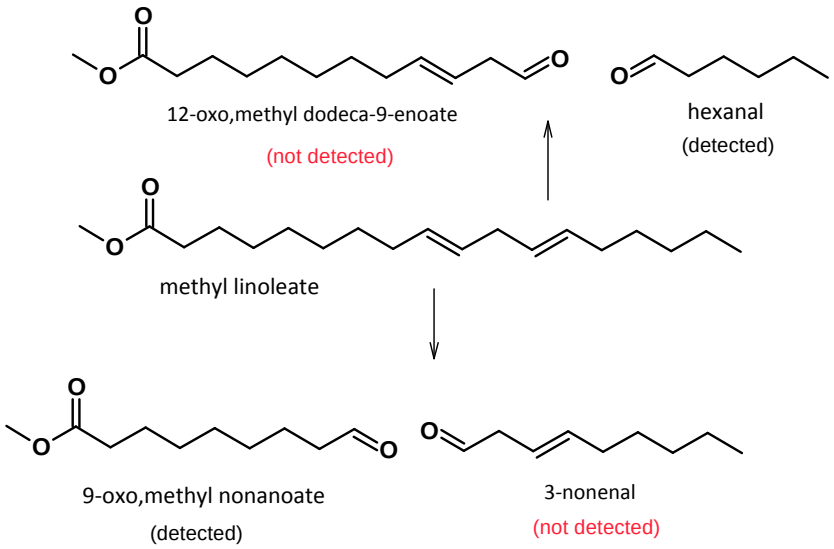

Figure 4: Structure of species which were expected from the Waddington mechanism for methyl linoleate.

Some species with a phenyl ring coming from the oxidation of benzene were detected. These species are toluene and phenol which are likely formed by ipso-addition to benzene of CH_3 radicals and O atoms. As for the n-decane/benzene blend oxidation study [27], these species are formed in very low amounts below 800 K (see Figure 3 for mole fraction profiles of phenol and toluene).

Mole fraction of reactants and all detected reaction products are given in Supplementary material. The selectivities of the measured products are given in Figure 5 at the temperatures corresponding to the maximum of conversion at low-temperature for each ester, i.e. 625 K for methyl stearate, 650 K for methyl oleate, and 700 K for methyl linoleate. For the three studied esters, the largest selectivity was obtained for carbon monoxide: 27% for methyl stearate, 37% for methyl oleate and 62% for methyl linoleate. For the saturated reactant, large selectivities were also obtained for formaldehyde (27%), acetaldehyde (14%), methanol (6.3%) and methylacrylate (5.8%). Other compounds, such as C_4–C_{16} 1-alkenes and C_5-C_{18} unsaturated methyl esters were produced in lower amounts (less than 2%). While CO_2 was formed in large amounts with unsaturated esters (selectivity of 7.3% for methyl oleate and 28% for methyl linoleate), its formation could not been seen below 800 K for methyl stearate. The important point which can be noted for unsaturated compounds is the particularly large selectivity spotted for products formed via the Waddington mechanism: i.e. nonanal and 9-oxo,methyl nonanoate for methyl oleate and hexanal and 9-oxo,methylnonanoate for methyl linoleate (see Figure 5).

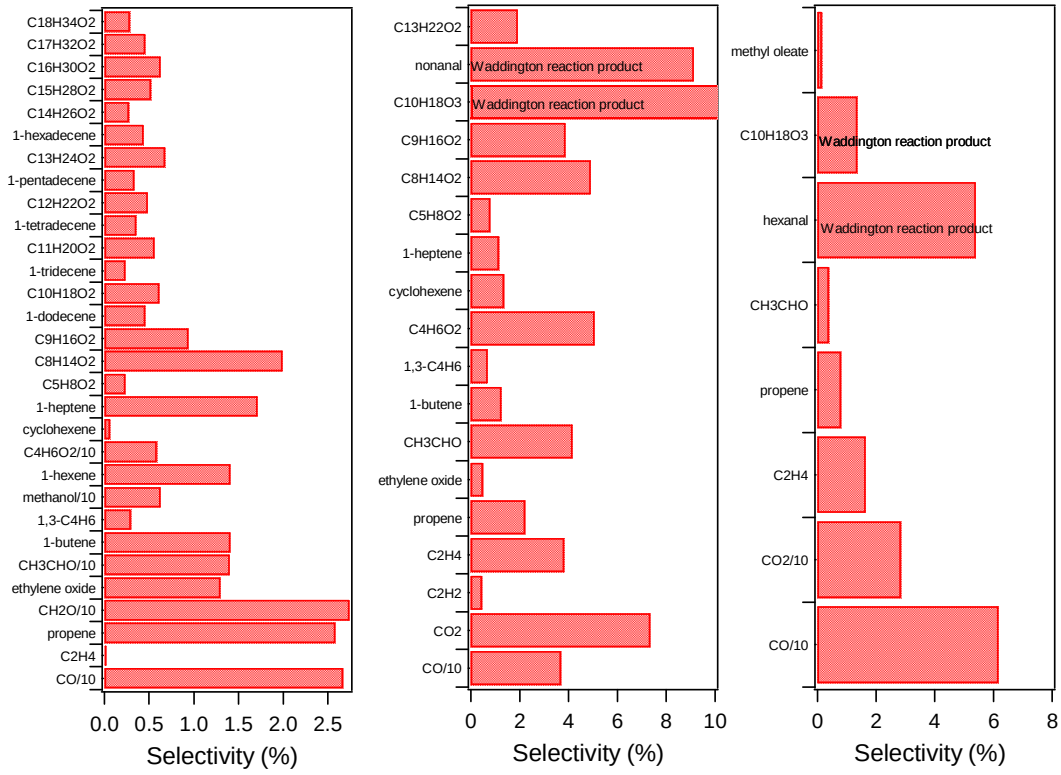

Figure 5: Product selectivity (related to the sum of the measured products) obtained during the JSR oxidation of the three methyl esters. Left panel: methyl stearate at 625 K (selectivity divided by 10 for CO, CH_2O, CH_3CHO, methanol and methyl acrylate). Center panel: methyl oleate at 650 K (selectivity divided by 10 for CO). Right panel: methyl linoleate at 700 K (selectivity divided by 10 for CO and CO_2).

4. Kinetic modeling: lumped kinetic scheme of biodiesel fuels

All the simulations discussed in this section are performed using the computational tools belonging to the OpenSMOKE++ library [36]. As already discussed in Saggese et al. [26], a lumped approach to the oxidation of heavy methyl esters allowed to extend the overall POLIMI kinetic mechanism by simply including ~60 new lumped species and ~2000 reactions. With respect to the more than 4800 species involved in the detailed kinetics by Westbrook et al. [5], there is a relevant saving in the overall dimensions of the scheme. As a matter of facts, instead of including in the kinetic scheme all the possible isomers of radicals and molecules, a few lumped species refers not only to several isomers with the same formula but also to adjacent homologous species. Intermediate species are split between the two closest reference species, with the lever rule [37]. For instance, intermediate species between methyl-decanoate ($C_{11}H_{22}O_2$) and methyl palmitate ($C_{17}H_{34}O_2$) are not included in the kinetic scheme. Then, the oxidation of methyl-myristate ($C_{15}H_{30}O_2$), not included in the scheme, is obtained through the corresponding oxidation of a molar mixture of 33% of methyl-decanoate and 67% of methyl-palmitate.

A further significant reduction of the number of involved species is obtained by assuming the steady state approximation [38] and [39] for the high temperature decomposition of large alkyl radicals. For these μ radicals the monomolecular decomposition and isomerization reactions largely prevail on other

bimolecular interactions with the reacting mixture. Therefore, they are directly transformed into their primary decomposition and isomerization products.

At low temperatures, large alkyl radicals can add to oxygen to form peroxy radicals. In the case of unsaturated methyl esters, the peroxy radicals formed on the allyl positions are less prone to isomerize to alkyl hydroperoxy radicals if a double bond is contained within the transition state intermediate, because of the very slow abstraction of the 1–5 vinyl hydrogen [5], [26] and [40].

Thus, the primary radicals of unsaturated methyl esters are lumped in two separate groups of radicals: the propagating and the allylic ones. The different low temperature reactivity of the unsaturated methyl-esters is likely due to several combined phenomena. On one part it is due to the favored decomposition of RO_2 peroxy radicals obtained from the addition of allylic fuel radicals to O_2 [41]. On the other part, it is due to the difficulty of several peroxy radicals of unsaturated methyl esters to isomerize and to follow a degenerate propagation path with the final formation of carbonyl-hydroperoxide species.

Figure 6 schematically describes the lumped scheme for the three esters with the name of main species as they appear in the model (as an example, MSTEA, MEOLE and MLINO correspond to methyl stearate, methyl oleate and methyl linoleate, respectively). Only methyl oleate and methyl linoleate can form the non-propagating allyl-type radicals.

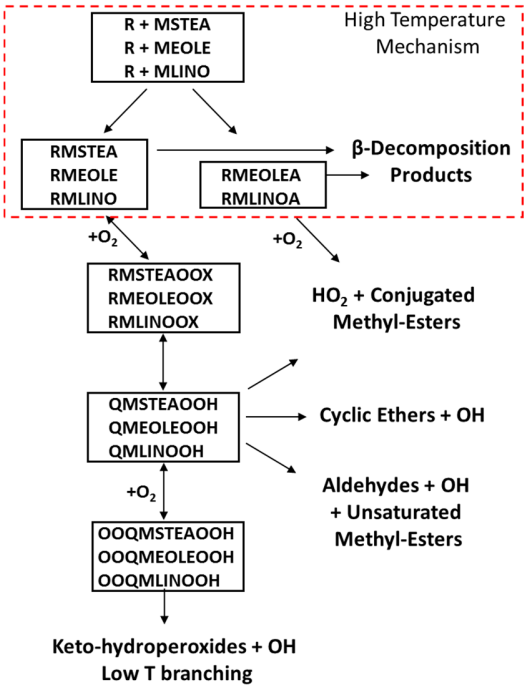

Figure 6: Lumped scheme for the three methyl-esters. Only methyl-oleate and methyl-linoleate can form the non-propagating allyl-type radicals: RMEOLEA and RMLINOA.

Additional details about the development of the lumped kinetic model of methyl esters can be found in previous papers [38], [39], [37] and [26]. In this work we slightly revised the model accounting for the new low temperature measurements. Table 5 summarizes the kinetic parameters used for some relevant reactions of heavy methyl esters. The new experimental data presented in this work allowed updating the

kinetic parameters originally proposed by Saggese et al. [26], especially for the low temperature conditions. The different degree of unsaturation is the main reason for the different tendency of the methyl-esters to form propagating and non-propagating allyl radicals. Moreover, also the radical decomposition and radical isomerization reactions have been slightly modified always maintaining a continuity and regularity among saturated and unsaturated methyl esters. The complete kinetic model, together with thermochemical and transport properties, is attached as Supplementary material to this paper.

Table 4: Kinetic parameters of heavy methyl-esters[a].

Reactions	**MPA** **Me-palmitate**	**MSTEA** **Me-stearate**	**MEOLE** **Me-oleate**	**MLINO** **Me-linoleate**	**MLIN1** **Me-linolenate**
Chain Initiation	2.4e17/83000	2.5e17/83000	2e16/74000 1e17/82000	2e16/74000 1e17/82000	2e16/74000 8e16/82000
H-abstractions to form R[b] **RA (non propagating allyl radicals)**	38/1 --	40/1 --	28/1 12/1	20/1 18/1	12/1 24/1
R→β-decomposition	4e13/30000	4e13/30000	2.8e13/30000	2.1e13/30000	2e13/30000
RA→β-decomposition	--	--	2e13/31000	0.7e13/30000	1e13/30000
O_2+R→ROO	2e9/0	2e9/0	2e9/0	2e9/0	2e9/0
O_2+R→HO_2+Unsaturated ME	1e9/2000	1e9/2000	1e9/2000	1e9/2000	1e9/2
ROO→O_2+R	5e13/30500	5e13/30500	5e13/31000	5e13/31000	5e13/31000
ROO→QOOH	1e12/24500	1e12/24500	1e12/25500	1e12/25500	1e12/25500
QOOH→ROO	2e10/16000	2e10/16000	2e10/17000	2e10/17000	2e10/17000
QOOH→HO_2+Unsaturated ME	3e12/24000	3e12/24000	3e12/24000	3e12/24000	3e12/24000
QOOH→OH+cyclic Ethers	1e10/14000	1e10/14000	1e10/14000		
QOOH→OH+aldehydes	2e12/22500	2e12/22500	2e12/22500	1.5e12/22500	3e12/22500
O_2+QOOH→OOQOOH	2e9/0	2e9/0	2e9/0	2e9/0	2e9/0
OOQOOH→O_2+QOOH	5e13/29500	5e13/29500	5e13/30000	5e13/30000	5e13/30000
OOQOOH→OH+Ketohydroperoxides	1e12/24500	1e12/24500	1e12/25000	1e12/25000	1e12/25000
Ketohydroperoxides→OH+….	--	1.5e16/43500	--	--	1.5e16/45000

[a] Kinetic parameters (A/E) refer to the Arrhenius expression k=A exp (-E/RT). Units are m, kcal, kmol, K, s

[b] Kinetic parameters of H abstraction reactions refer to the number and type of equivalent H atoms (n_H/type)

The chemistry used in the present lumped model for the oxidation of benzene comes from a recently revised benzene oxidation mechanism [42]. This revised model was tested against many literature data, including also experimental data for a mixture of benzene and *n*-decane under similar conditions [27], as also reported in the Supplementary material (Figures S3 and S4).

4.1. Waddington mechanism

A further difference between saturated and unsaturated methyl esters is related to the so called Waddington mechanism [43]. An hydroxyl peroxy alkyl radical, formed through the OH addition to the double bond of unsaturated methyl-esters and a subsequent oxygen addition, can form OH and two carbonyl products. Figure 4 shows the possible reaction path to form hexanal and 12-oxo,methyl dodeca-9-enoate from methyl-linoleate. Similarly, it is also possible to form 3-nonenal and 9-oxo,methyl nonanoate. More unsaturated carbonyl components are obtained with Waddington mechanism from methyl-linolenate.

Waddington Mechanism was included in the kinetic scheme by using the kinetic parameters suggested by Mehl et al. [44] and Sun et al. [45]. This inclusion (always with a lumped approach) only required a few new reactions and species, without a relevant increase of model dimension. Our goal was to verify their effect in the analyzed experimental conditions.

Only a couple of the different reaction paths have been included. The first is the methyl-oleate forming nonanal and 9-oxo,methyl nonanoate (Figure 7). The second one is the methyl-linolenate forming hex-3-enal and 12-oxo,methyl dodeca-9-enoate (Figure 8). The introduction of the lumped Waddington mechanism required the introduction of the 8 new lumped species shown in Table S1 of the Supplementary material. Thermodynamic properties (stored under the form of NASA polynomial coefficients) were calculated using software Thergas [46] (based on group additivity method proposed by Benson [47] with group values from references [47] and [48]).

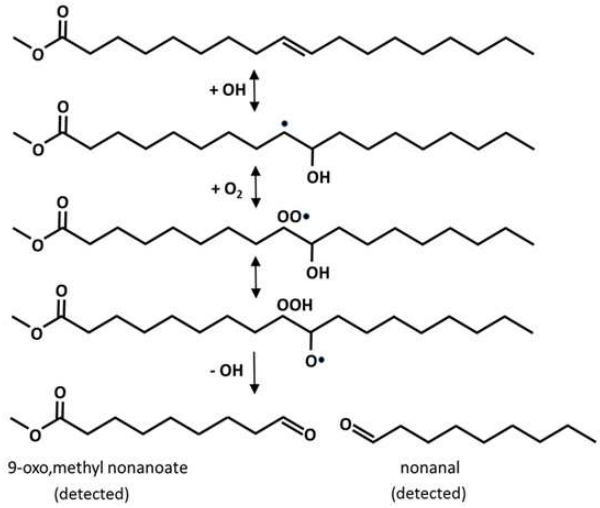

Figure 7: Waddington mechanism: methyl-oleate forming nonanal and 9-oxo,methyl nonanoate.

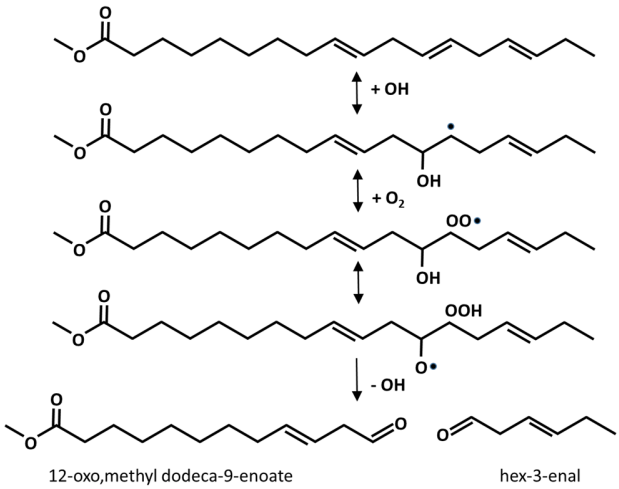

Figure 8: Waddington mechanism: methyl-linolenate forming hex-3-enal and 12-oxo,methyl dodeca-9-enoate.

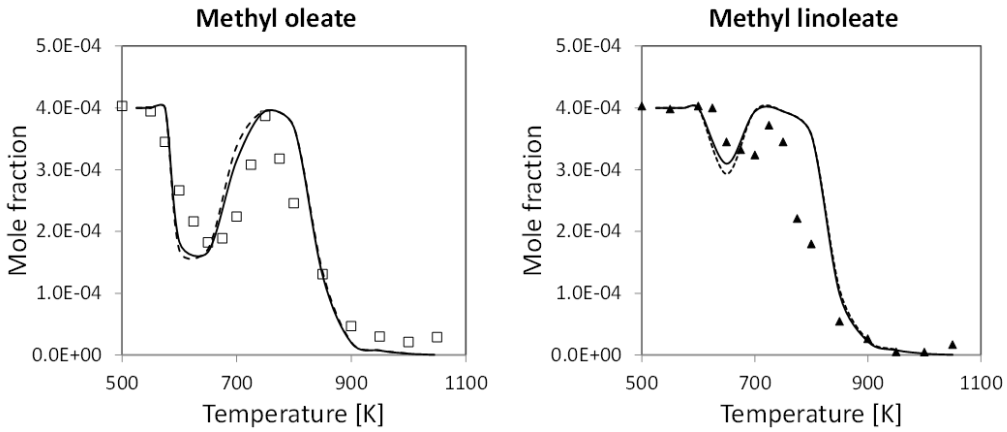

Figure 9: Mole fractions of methyl-oleate and methyl-linoleate. Comparisons of experimental data (symbols) and model predictions with (solid lines) and without Waddington mechanism (dashed lines).

Figure 9 shows the limited effect of Waddington mechanism taking place at temperatures between 600 and 700 K under the conditions of the present study. For these reasons and following a lumped approach, only the two reaction paths of Figures 7 and 8, and corresponding intermediate products, are accounted for. Moreover, the Waddington reactions and products of methyl-linoleate are simply obtained as a linear combination of the ones of methyl-oleate and methyl-linolenate.

4.2. Four and six center molecular decompositions

Under the conditions of this study, four and six center molecular decompositions are of notable importance at temperatures higher than 750 K. Figure 10 shows a schematic example of the possible formation of 1,3-butadiene and methyl-tetradecanoate from methyl-linoleate through a 6-membered ring transition state as well as the formation of methyl 7-octenoate and 1-decene from methyl-linoleate through a 4-membered ring transition state.

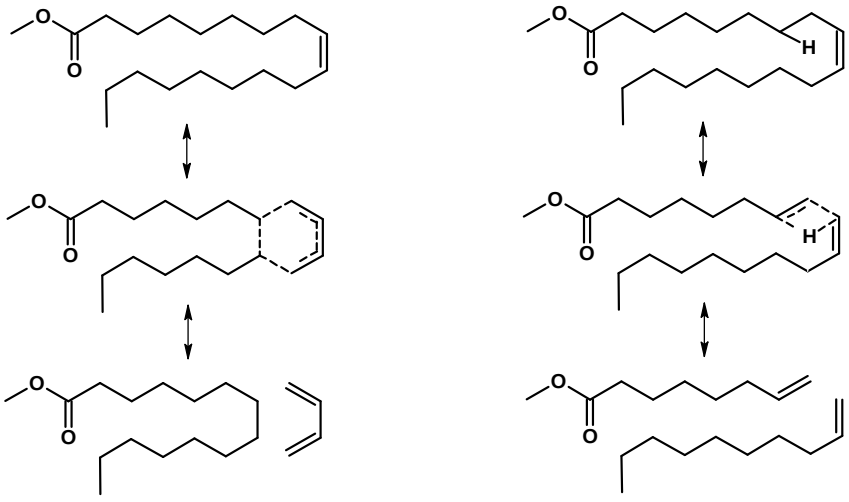

Figure 10: Example of four and six center molecular decompositions of methyl-linoleate.

There are a large number of possible reactions belonging to this class and they can explain the formation of butadiene, dialkenes and alkenes from unsaturated methyl esters. Again only a few lumped reactions to form butadiene, ethylene and propene have been included in the kinetic scheme. The kinetic parameters ($2 \cdot 10^{12} \exp(-50000[\text{cal mol}^{-1}]/RT)$ [s^{-1}]) are derived from similar molecular reactions of alkenes and dialkenes [49] and [50]. Figure 11 shows how these reactions are significant to explain butadiene formation at 800–900 K for unsaturated reactants.

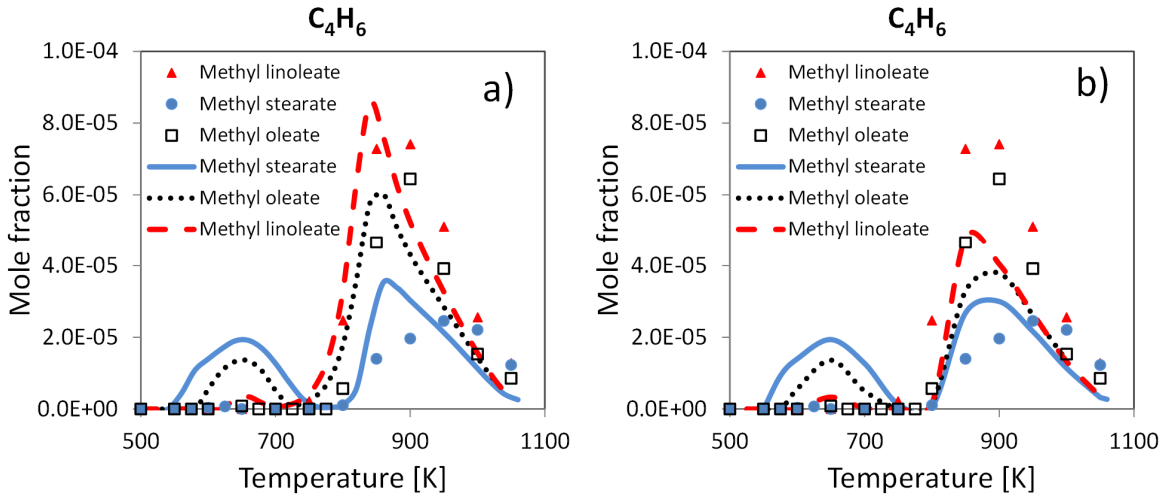

Figure 11: Effect of molecular reactions on butadiene formation from unsaturated methyl esters. (a) Complete kinetic scheme. (b) Kinetic scheme without these molecular reactions. Experimental measurements (symbols), model predictions (lines).

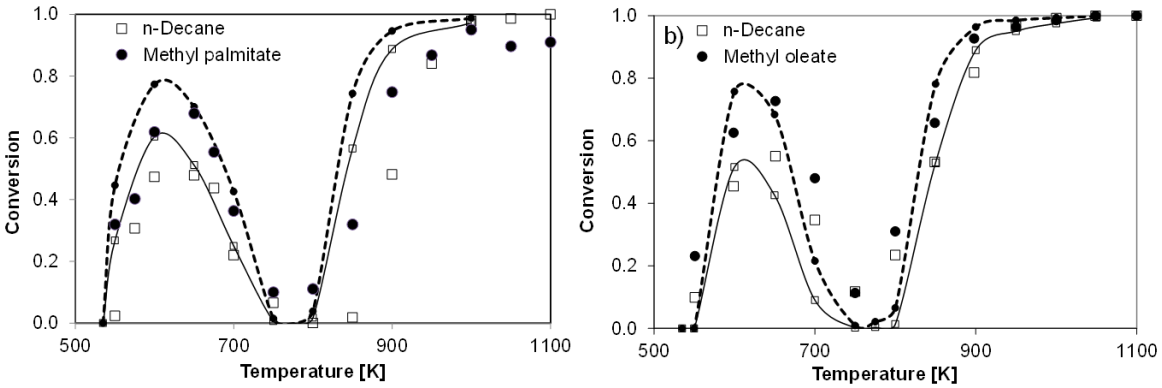

Figure 12: Conversion at atmospheric pressure obtained during the stoichiometric oxidation of n-decane mixtures at 1.5 s: panel (a) with 26% methyl-palmitate [19], panel (b) with 26% methyl-oleate [20] (xfuel=0.002xfuel=0.002, dilution in helium). Comparison of experimental (symbols) and predicted conversions (lines).

Figure 1 shows a comparison between model predictions and experimental fuel mole fraction profiles. The model properly captures the different reactivity of methyl esters at low-temperatures, methyl-linoleate being the least reactive and the saturated methyl stearate being the most reactive. At temperatures higher than 800 K, all the fuels convert in a very similar way, again confirming the experimental behavior.

Figure 1, Figure 2 and Figure 3 present the comparison between model predictions and experimental mole fraction profiles. Overall the model well reproduces mole fractions of reaction products in the high-temperature region (e.g., ethylene, formaldehyde, propene, 1-butene, 1,3-butadiene, methyl acrylate in Figure 2, methyl-heptenoate, toluene and phenol in Figure 3). An over-estimation is observed for small very unsaturated species (Figure 2) and methyl crotonate, methyl decenoate and 1-heptene, in Figure 3. CO and CO_2 mole fractions are well reproduced up to 1000 K. Above this temperature, CO mole fractions are slightly over-estimated whereas the opposite trend is observed for CO_2, showing the tendency to underestimate the system reactivity under these conditions (Figure 2). As already discussed in Saggese et al. [42], the observed over-estimations of acetylene, propyne and allene are mainly due to the benzene chemistry and namely to the successive decomposition reaction of benzoquinone radicals ($C_6H_3O_2$). These deviations could suggest useful extensions of the lumped benzene scheme, including more details in this decomposition path.

At low-temperatures, a very good agreement is obtained for formaldehyde and methyl acrylate (Figure 2). The model tends to overpredict the mole fraction of other reactions products. This can be seen for ethylene (Figure 2) and methyl crotonoate (Figure 3), as an example. This is largely due to the lumping strategy, i.e. large species with the same skeleton as the reactant are voluntary omitted and the decomposition reactions into small species are then privileged. Finally, Figure 2 shows that the profiles of CO and acetaldehyde are shifted towards higher temperatures for methyl stearate relatively to the unsaturated methyl esters. However, it is difficult to explain such a behavior, not reproduced by the model.

A correct agreement is obtained (better than a factor of 3) for the three Waddington reaction products detected in the present study (hexanal, nonanal and 9-oxo methyl nonanoate in Figure 3). Be aware that the computed profile for hexanal shown in Figure 3 is actually that of hexenal due to the lumping strategy (the Waddington reactions and products of methyl-linoleate are simply obtained as a linear combination of the ones of methyl-oleate and methyl-linolenate).

5. Model validation and comparisons with literature experimental measurements

As already mentioned in this paper, the literature is still rather scarce as far as experimental data useful for model validation are concerned. The model validation refers to the following different sets of data:

- Stoichiometric air oxidation of *n*-decane mixtures with 26% methyl palmitate [19] and with 26% methyl oleate [20] in an atmospheric pressure JSR.
- Oxidation of rapeseed methyl ester (RME) in a JSR at 1 and 10 atm [18].
- Shock tube experiments with different methyl esters:
  - Stanford experiments [13] and [16] at 7 atm.
  - Rensselaer experiments [14] and [51] at 10 and 20 atm.

5.1. Oxidation of *n*-decane mixtures with methyl palmitate [19] and methyl oleate [20] in an atmospheric pressure JSR

Figure 12 shows a sample of comparison between experimental data and model predictions for the stoichiometric oxidation of n-decane mixtures including 26% of methyl-palmitate [19] or methyl-oleate [20], respectively. The reactivity of these systems is largely driven by *n*-decane oxidation, thus they are not completely useful to evaluate the low temperature reactivity specific to esters. Detailed comparisons with

the major products from the oxidation of the *n*-decane/methyl-oleate mixture are reported in the Supplementary material (Figure S1).

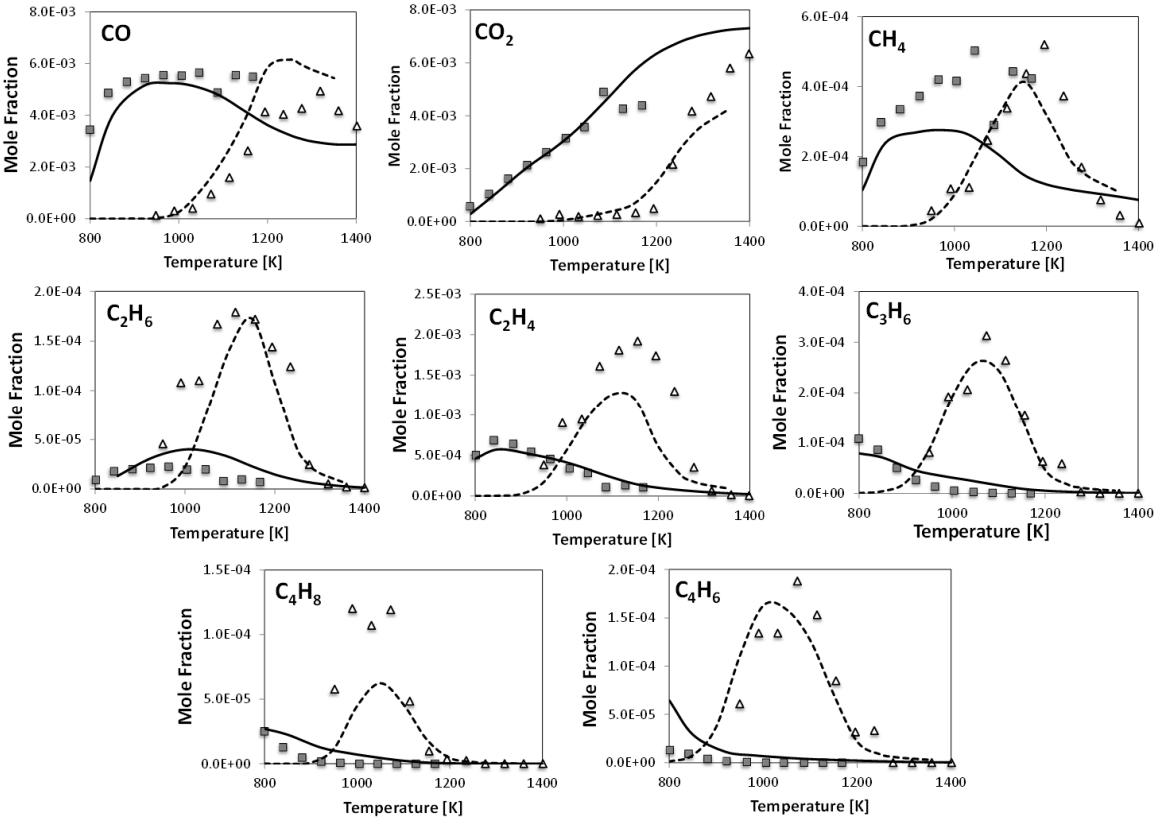

Figure 13: Stoichiometric oxidation of rapeseed methyl ester [18]. Comparisons of experimental data (1 atm and 0.07 s: triangles; 10 atm and 1 s: squares) and model predictions (lines).

5.2. Oxidation of rapeseed methyl ester (RME) in a JSR at 1 and 10 atm [18]

The oxidation of rapeseed methyl ester was studied by Dagaut et al. [18] in the Orléans JSR, at temperatures from 800 to 1400 K, different equivalence ratios, and pressures of 1 and 10 atm. All the experiments used highly diluted RME (0.05% fuel)/O_2/N_2 mixtures. According to the experimental data, the following RME composition (mole fractions) was assumed: 0.043 palmitate, 0.013 stearate, 0.600 oleate, 0.211 linoleate and 0.132 methyl linolenate. Figure 13 shows that a reasonable agreement between predictions and experimental data can be obtained using the present model. The model well reproduces the pressure effect on the formation of reaction products, especially the shift of the maximum mole fraction of species towards lower temperatures due to a higher reactivity when the pressure is increased.

5.3. Shock tube ignition delay times for different heavy methyl esters

5.3.1. Stanford experiments at 7 atm

Ignition delay times for different methyl-esters were recently measured behind reflected shock waves, using an aerosol shock tube at Stanford [16]. Methyl-decanoate, methyl-laurate ($C_{13}H_{26}O_2$), methyl-

myristate ($C_{15}H_{30}O_2$), and methyl-palmitate ($C_{17}H_{34}O_2$) were analyzed, together with a blend of methyl oleate ($C_{19}H_{36}O_2$) with 30% FAME. Experiments were conducted in 4% oxygen/argon mixtures, at temperatures from 1026 to 1388 K, a pressure of 7.0 atm, and equivalence ratios of 0.75 and 1.25. The oxidation of methyl decanoate ($C_{11}H_{22}O_2$) was also studied and well compared with previous experimental data [51]. Figure 14 shows a comparison of the experimental ignition delay times with the model predictions for different methyl esters. As already mentioned, on the basis of a vertical lumping, only methyl decanoate (MD), methyl palmitate (MPA), and methyl-stearate (MSTEA) are assumed as reference species of large saturated methyl esters. Intermediate species are derived with the lever rule; thus the following MD/MPA mixtures identically represent methyl laurate (MLA = 2/1) and methyl myristate (MMY = 1/2). The reliability of the vertical lumping is supported by the fact that the structures of MD, MLA, MMY, and MPA are identical except that the carbon chain length moves from 10 for MD up to 16 for MPA. A comparison among these sets of data reveals that ignition delay time slightly and progressively decreases as the carbon chain length increases from MLA to MPA. Figure 14 further confirms the reliability of the lumped model of methyl esters, also in comparison with the experimental data of MLA and MMY, as well as with the data of methyl oleate and methyl linoleate of Campbell et al. [13].

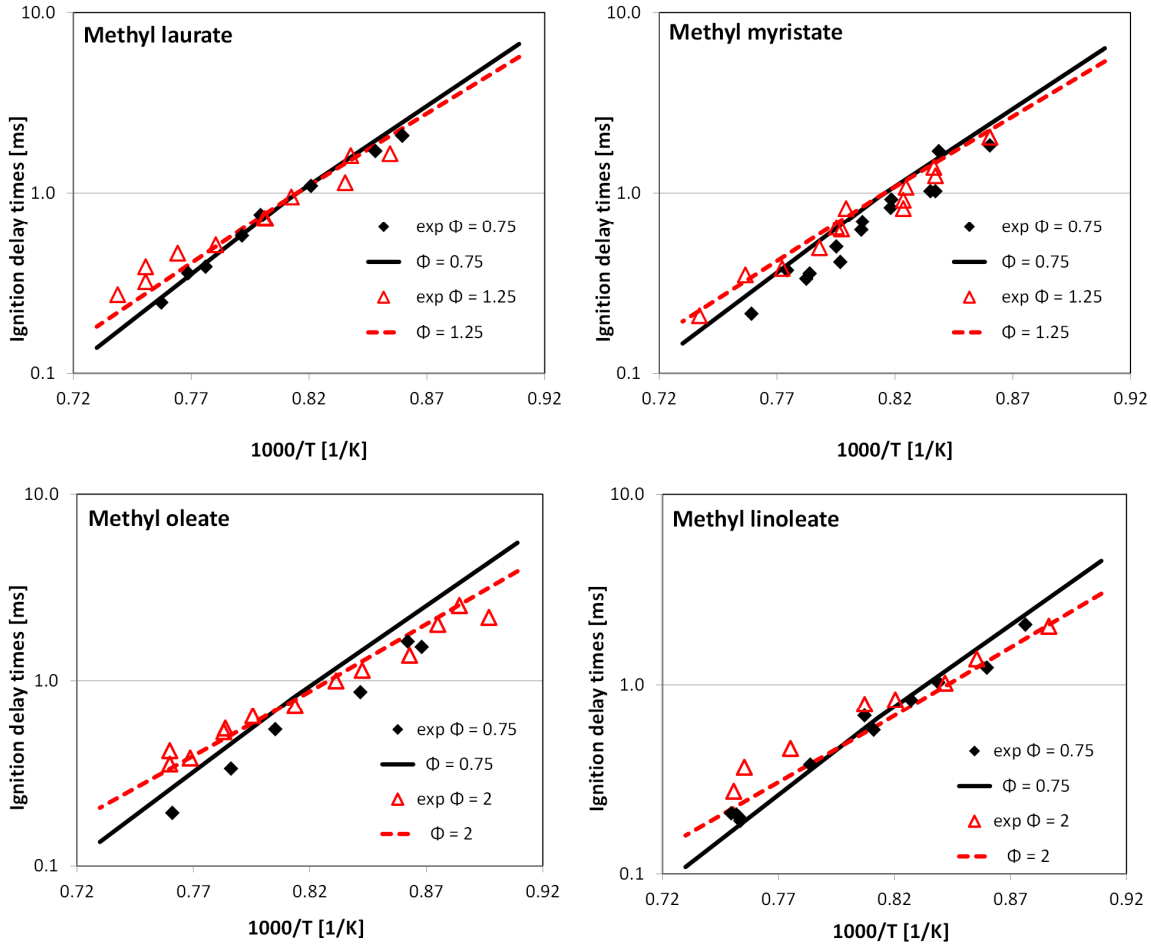

Figure 14: Methyl ester ignition delay times in 4% oxygen/argon mixtures, at 7 atm, and different equivalence ratios. Comparison of experimental data [13] and [16] (symbols) and model predictions (lines).

It was experimentally observed that the apparent activation energy decreases as equivalence ratio increases, as shown in Figure 14, for all these ester fuels. This fact is a significant evidence that the chemistry controlling ignition in the rich methyl oleate blends is different than at lean ratios [13]. This effect is here discussed using methyl-linoleate as an example.

At temperatures lower than 1200 K, the chemistry controlling ignition is the same under rich and lean conditions. Since these mixtures have the same amount of O_2 (4%), the rich mixtures ignite faster due to the higher fuel concentration. The opposite behavior is observed at high temperatures, where lean mixtures ignite faster. As a result, a higher apparent activation energy can be observed under lean conditions.

This behavior is due to the relative importance of pyrolysis and oxidation reactions. At high temperatures (above 1200 K), the fuel is mostly consumed by endothermic pyrolysis reactions before ignition. For this reason, there is a temperature reduction especially for the rich mixtures. Figure 15 shows that at 1370 K there is a cooling of ~25 K under rich conditions and only ~10 K under lean conditions, due to the lower amount of fuel. On the contrary, this endothermic effect is not observed at low temperatures, due to the lower importance of pyrolysis reactions. Note that the important role of oxidation reactions at low temperatures (1100 K) is also confirmed by the sensitivity analysis of Figure 15, where reactions of OH and HO_2 are very sensitive.

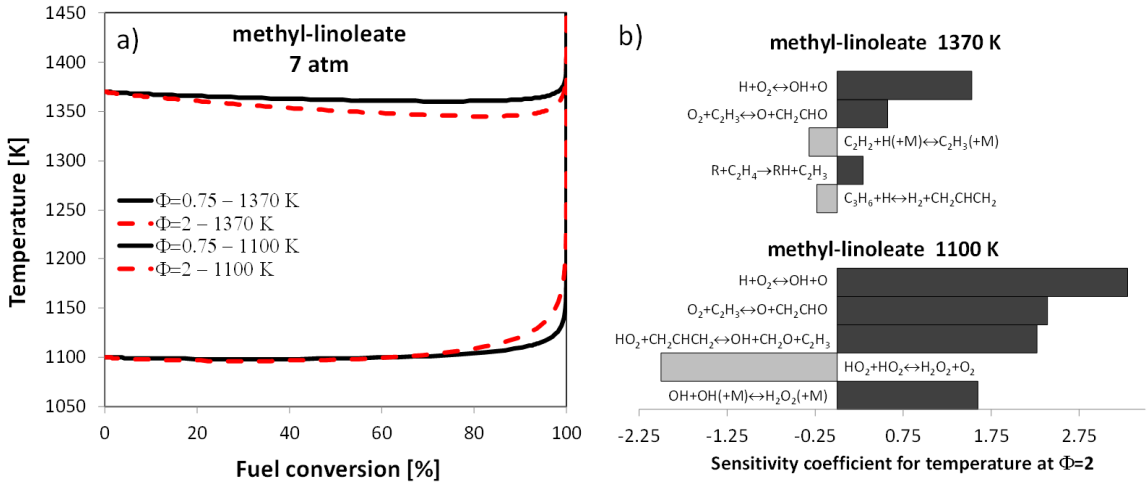

Figure 15: Panel (a): Predicted temperature as function of the fuel conversion for methyl-linoleate at 7 atm and two initial temperatures and two equivalence ratios. Panel (b): Sensitivity analysis for the two initial temperatures. Negative sensitivity coefficients indicate the reactions that decrease the reactivity.

5.3.2. Rensselaer experiments at 10 and 20 atm

Very recent data of Wang et al. [14] at 950–1350 K deal with the ignition of palmitate, stearate, oleate and linoleate. Figure 16 shows a comparison of the ignition delay times of saturated and unsaturated methyl-esters: methyl-stearate, methyl-oleate, and methyl-linoleate. The behavior of the three fuels is very similar at high temperatures, while methyl-stearate shows a more pronounced tendency towards low temperature reactivity at temperatures lower than 1000 K. According to Wang recommendations, these simulations are also accounting for the effect of dP/dt (in the order of 2–3% m s^{-1}), due to viscous gas dynamics. Finally, Figure 17 shows further comparisons between experimental ignition delay times of

methyl-palmitate at variable pressure and equivalence ratios. The model properly captures the experimental trends, even if these comparisons indicate a slight overestimation of the ignition delay times at 10 atm.

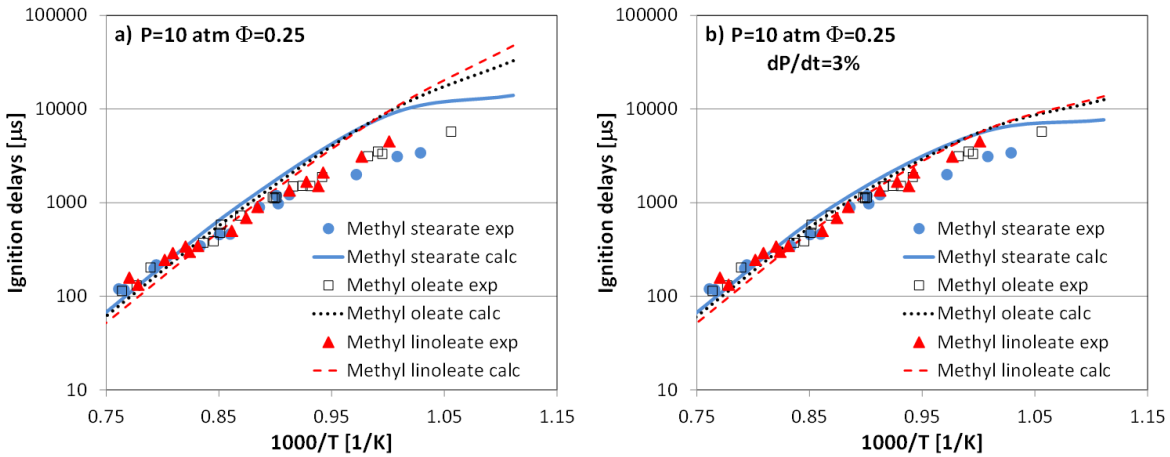

Figure 16: Ignition delay times of methyl-stearate, methyl-oleate, and methyl-linoleate. Experimental measurements (symbols) [14], model predictions (lines).

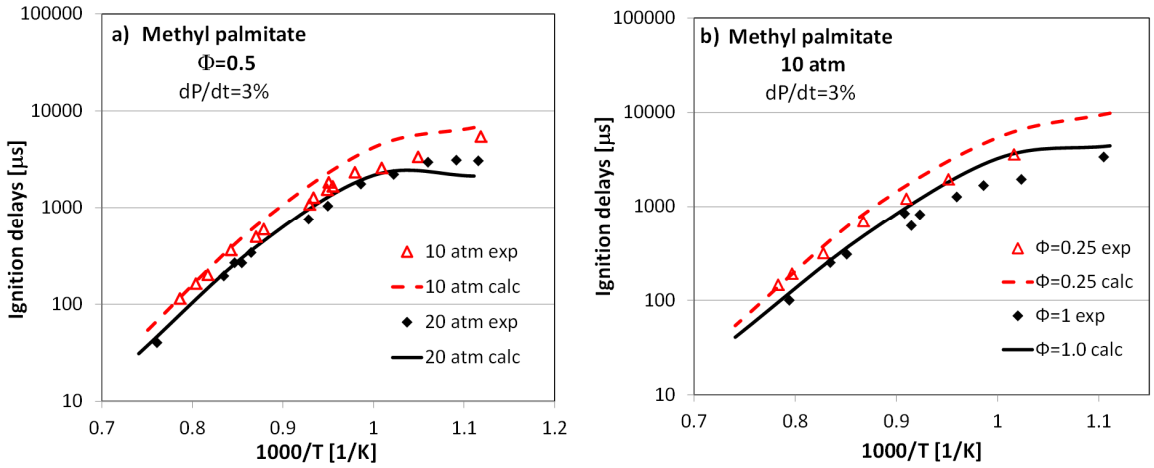

Figure 17: Ignition delay times of methyl-palmitate. Panel (a): Pressure effect. Panel (b): Effect of the equivalence ratio at 10 atm. Experimental measurements [14] (symbols), model predictions (lines).

6. Kinetic discussion

The lumped kinetic model was used to compare the reactivity of the five main esters (palmitate, stearate, oleate, linoleate and linolenate) present in biodiesel fuels, both in an atmospheric JSR and in a shock tube device at 13.5 atm. These conditions are similar to those used by Westbrook et al. [5] to do predictive comparisons in their previous work about methyl esters oxidation (see Figure S2 in Supplementary material). Panels (a) and (b) of Figure 18 shows predictions obtained by a couple of five separate simulations, each with a different methyl ester fuel, using the present model. Note that both models have not been validated for methyl linolenate as no experimental data are available to our knowledge and that data computed for this species should be regarded with hindsight.

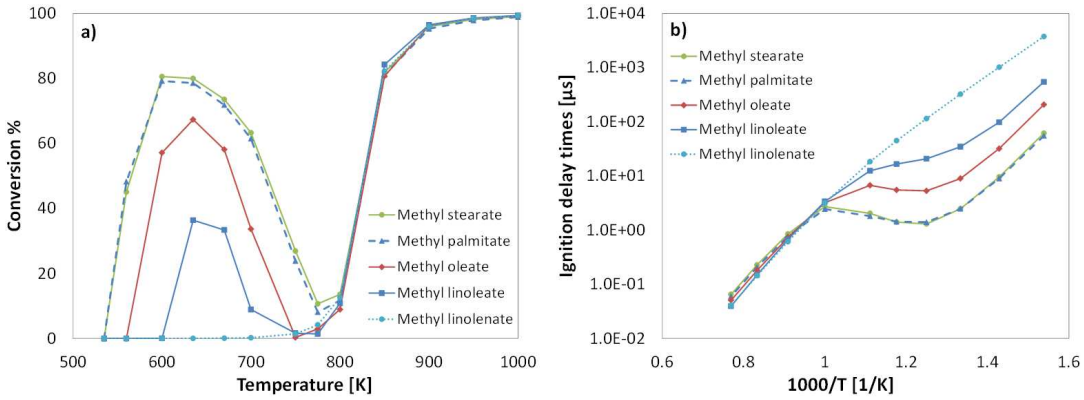

Figure 18: Calculated relative reactivity of the five main esters of biodiesel fuels. (a) JSR at 1 atm, 1.5 s, 0.2% fuel at Φ = 1, with He diluent. (b) Shock tube device, air/fuel mixtures in stoichiometric conditions, at 13.5 atm.

While methyl-palmitate and methyl-stearate behave in a very similar way under both conditions, the effect of the unsaturation under low temperature conditions is well confirmed, with a significant reactivity decrease when the number of unsaturation increases. Finally, it is important to highlight the complete absence of NTC or low temperature reactivity, both in a JSR and in a shock tube, for methyl-linolenate, a compound including three unsaturations.

Predictive simulations give fuel mole fraction profiles somewhat different from those obtained by Westbrook et al. [5]. This model was only tested against the few data that were available at the time they wrote their paper (JSR data for methyl palmitate, oleate in mixture with n-decane and rapeseed oil methyl ester [18], [19] and [20]). As an example, in a JSR, the present model predicts a more pronounced NTC behavior for methyl palmitate, stearate, oleate and linoleate than the previous model of Westbrook et al. (especially for methyl oleate which had a minimum conversion of 50% at the end of the NTC region). Another difference is the shift of the temperature at which the maximum conversion is observed for methyl linoleate (700 K with Westbrook et al. model against 625 K with the present model). As far as methyl linolenate is concerned, the present models predicts almost no reactivity below 750 K whereas the model of Westbrook et al. predicts an increase of the reactivity from 650 K with a plateau up to 750 K and then the usual increase of the conversion due to the high temperature oxidation chemistry. None of these models have been tested against methyl linolenate continuous flow reactor experimental data, since these data are not currently available.

For shock tube data, the relative positions of ignition delay time curves are similar with both models. The present model predicts no NTC behavior for methyl linolenate (as in a JSR), whereas the model of Westbrook et al. computes a slight one. A major difference in the computed data is the position of the minimum of reactivity at the end of the NTC. It is located at about 900 K for all fuels (except methyl linolenate for which there only a slight inflection) according the model of Westbrook et al.. With the present model, the minimum is located at 900 K for methyl oleate and it is shifted towards higher temperature (T = 1000 K) for the two saturated methyl esters.

Figure 19 shows the sensitivity analysis for methyl-stearate, methyl-oleate and methyl-linoleate, in the JSR conditions, at 650 and 850 K, whereas Figure 20 displays a rate-of-production analysis at 650 K for the three fuels.

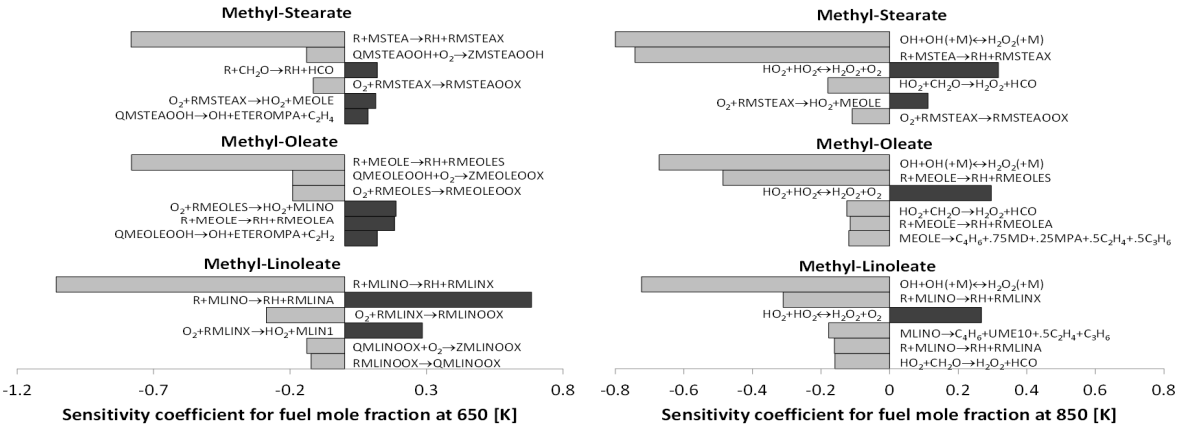

Figure 19: Sensitivity analysis for methyl-stearate, methyl-oleate and methyl-linoleate, in the JSR conditions at 650 K and 850 K. Negative sensitivity coefficients indicate the reactions that increase the reactivity.

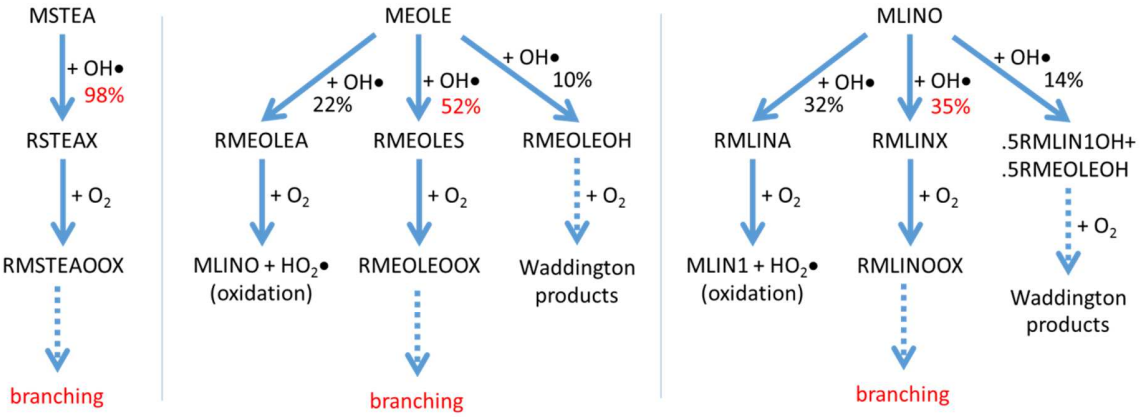

Reactant	MSTEA	MEOLE	MLINO
Branching steps	98	52	35
Sum of propagating steps	-	32	46
• Oxidation of allylic radicals	-	22	32
• Waddington mechanism	-	10	14

Figure 20: Rate-of-production analysis for methyl-stearate, methyl-oleate and methyl-linoleate, in the JSR conditions at 650 K.

These figures clearly explain the reasons of the difference in reactivity between the three ester fuels at low temperatures. According to the sensitive analysis, the H-abstraction reactions from unsaturated fuels to form the non-propagating allyl type radicals (R + MEOLE → RH + RMEOLEA for methyl oleate and R + MLINO → RH + RMLINA for methyl linoleate) have a positive coefficient, thus indicating a clear inhibiting effect on the reactivity of the system. These reactions do not exist for methyl stearate (as there is no C=C double bond) which was the most reactive species. It is also interesting to compare the ratio of the sensitivity coefficients of the two types of H-atom abstractions (when relevant) to compare their relative effect. For methyl oleate, the sensitivity coefficient of the H-abstraction reactions leading to the non-propagating allyl type radicals (inhibitive) is about a quarter of the sensitivity coefficient of the H-

abstraction reactions forming non allyl type radicals (promoting). For methyl linoleate, the ratio increases abruptly to about 2/3, confirming the strong inhibiting effect due to the presence of the two double bonds in the alkyl chain). At 850 K (high temperature region), all the H-abstraction reactions have negative sensitivity coefficients. The three fuels react in a very comparable way (as it was seen in experiments) and also the sensitivity analysis confirms this similarity.

Another class of reactions having an inhibiting effect in the reactivity at low temperature are reactions of fuel radicals with molecular oxygen to form the corresponding unsaturated esters and HO_2 (O_2 + RMSTEAX → HO_2 + MEOLE, O_2 + RMEOLES → HO_2 + MLINO, and O_2 + RMLINX → HO_2 + MLIN1). The sensitivity analysis also showed that the decomposition of alkyl-hydroperoxyl radicals to form cyclic-ethers has an inhibitive effect (QMSTEAOOH → OH + ETEROMPA + C_2H_4, and QMEOLEOOH → OH + ETEROMPA + C_2H_2).

The relative increasing importance of inhibiting propagation paths (oxidation of allylic radicals and Waddington reactions which do not exist for methyl stearate) with the number of double bonds in the fuel is confirmed by the rate-of-production analysis performed at 650 K (Figure 20): the part of the branching falls from about 98% to 52% and 35% from methyl stearate to methyl oletate and methyl linoleate, respectively. Note that the Waddington mechanism is responsible for 10% and 14% of the fuel consumption for methyl oleate and methyl linoleate, respectively.

Finally, the sensitivity analysis further confirms the negligible reactivity of benzene up to 850 K. Only at higher temperature benzene and phenoxy radical reactions appear among the sensitive reactions. This confirms well the hypothesis that the JSR reactivity at low temperatures of the investigated esters was not influenced by the presence of benzene.

7. Conclusion/comments

This paper presents new experimental data for the oxidation in a jet-stirred reactor of methyl esters actually found in biodiesel fuel, methyl stearate, methyl oleate and methyl linoleate, over a wide range of conditions covering both the low- and high-temperature regimes. This is the first study with quantitative information highlighting the large differences of reactivity of these species in the low-temperature region, thanks to the use of benzene as a solvent with a very low reactivity in this temperature zone (below 850 K). Experimental observations confirm that the reactivity at low-temperature significantly decreases with the number of double bonds in the fuel molecule.

Many reaction products have been analyzed using gas chromatography (e.g., olefins, methyl esters with a double bond at the end of the chain produced from reactions of decomposition by β-scission, more specific species formed from the reaction of unsaturated compounds, such as aldehydes through the Waddington mechanism). However, due to the low concentration of biofuels at the inlet of the reactor, it was not possible to observe all expected low-temperature products as in previous studies [19] and [20] (e.g., cyclic ethers) because these species were formed in amounts below the detection limit.

A lumped mechanism previously developed for the oxidation of methyl esters has been further refined to better account for experimental observation. Main improvements concern the inclusion of species and reactions for taking into account the Waddington mechanism. The sensitivity analysis of the model shows that this class of reactions has almost no effect on the reactivity for methyl oleate but a more pronounced inhibiting effect for methyl linoleate. Another improvement of the model consists in considering the concerted (or molecular) decomposition of olefins to smaller unsaturated molecules as 1,3-butadiene. The analysis of the model showed that the this class of reactions only plays a role at high temperature (above

800 K) which is consistent with the relatively high activation barrier of this reaction type (~50 kcal mol^{-1}). Molecular reactions could require further kinetic investigations.

The lumped kinetic model, containing 18,217 reactions involving 461 species, has been tested over a wide range of conditions including jet-stirred reactor and shock tube data. The agreement between computed and experimental data is satisfactory with a correct prediction of the reactivity, especially at low-temperature where the three fuels studied in the present work exhibit large difference in reactivity. The reactivity agreement is also very good at high-temperature as it has been seen from shock tube and jet-stirred reactor experiments. Overall JSR reaction products mole fractions are well reproduced by the model. Discrepancies are observed for some of them (over-estimation at low-temperature, as for ethylene) which can be attributed to the lumping strategy employed to limit the size of the model (global decomposition into small species).

The effect of the C=C double bonds on the ignition delay times of methyl esters at low temperatures was already discussed by Westbrook et al. [41] and [52]. This effect and the differences among the unsaturated methyl-esters are here further verified with the new experimental data obtained in the jet stirred reactor. On the contrary, the similarity in ignition delay times for all methyl ester fuels at high-temperatures, irrespective of the variations in organic structure, was discussed and observed by Wang et al. [14]. In addition, these JSR experiments further confirm this behavior. In contrast, Das et al. [15] observed that unsaturated methyl esters with the C=C double bond nearest the carbonyl group had lower a sooting tendency than compounds where the C=C double bond was further along the carbon backbone. The dependence of the sooting tendencies on ester chemical structure confirms the complexity of the chemical mechanisms involved, and shows that this is an important area for further research activities.

Acknowledgment

This work was supported by European Commission ("Clean ICE" ERC Advanced Research Grant, Project No: 227669) and by the COST ActionsCM0901 (Detailed chemical kinetic models for cleaner combustion) and CM1404 (Chemistry of Smart Energy Carriers and Technologies – SMARTCATS). Authors acknowledge useful discussions with Prof. Mario Dente.

References

[1] K.T. Lee, S. Lim, Y.L. Pang, H.C. Ong, W.T. Chong, Integration of reactive extraction with supercritical fluids for process intensification of biodiesel production: Prospects and recent advances, Prog. Energy Combust. Sci. 45 (2014) 54–78.

[2] G. Knothe, Biodiesel and renewable diesel: A comparison, Prog. Energy Combust. Sci. 36 (2010) 364–373.

[3] M. Jesus Ramos, C. Maria Fernandez, A. Casas, L. Rodriguez, A. Perez, Influence of fatty acid composition of raw materials on biodiesel properties, Bioresour. Technol. 100 (2009) 261–268.

[4] L. Coniglio, H. Bennadji, P.A. Glaude, O. Herbinet, F. Billaud, Combustion chemical kinetics of biodiesel and related compounds (methyl and ethyl esters): Experiments and modeling – Advances and future refinements, Prog. Energy Combust. Sci. 39 (2013) 340–382.

[5] C.K. Westbrook, C.V. Naik, O. Herbinet, W. Pitz, M. Mehl, S.M. Sarathy, et al., Detailed chemical kinetic reaction mechanisms for soy and rapeseed biodiesel fuels, Combust. Flame. 158 (2011) 742–755.

[6] J.Y.W. Lai, K.C. Lin, A. Violi, Biodiesel combustion: Advances in chemical kinetic modeling, Prog. Energy Combust. Sci. 37 (2011) 1–14.

[7] P. Dievart, S.H. Won, J. Gong, S. Dooley, Y. Ju, A comparative study of the chemical kinetic characteristics of small methyl esters in diffusion flame extinction, Proc. Combust. Inst. 34 (2013) 821–829.
[8] K. Zhang, C. Togbe, G. Dayma, P. Dagaut, Experimental and kinetic modeling study of trans-methyl-3-hexenoate oxidation in JSR and the role of C=C double bond, Combust. Flame. 161 (2014) 818–825.
[9] Y.L. Wang, D.J. Lee, C.K. Westbrook, F.N. Egolfopoulos, T.T. Tsotsis, Oxidation of small alkyl esters in flames, Combust. Flame. 161 (2014) 810–817.
[10] S. Deng, J.A. Koch, M.E. Mueller, C.K. Law, Sooting limits of nonpremixed n-heptane, n-butanol, and methyl butanoate flames: Experimental determination and mechanistic analysis, Fuel. 136 (2014) 122–129.
[11] X. Yang, D. Felsmann, N. Kurimoto, J. Krueger, T. Wada, T. Tan, et al., Kinetic studies of methyl acetate pyrolysis and oxidation in a flow reactor and a low-pressure flat flame using molecular-beam mass spectrometry, Proc. Combust. Inst. 35 (2015) 491–498.
[12] Z. Zhang, E. Hu, C. Peng, X. Meng, Y. Chen, Z. Huang, Shock Tube Measurements and Kinetic Study of Methyl Acetate Ignition, Energy Fuels. 29 (2015) 2719–2728.
[13] M.F. Campbell, D.F. Davidson, R.K. Hanson, C.K. Westbrook, Ignition delay times of methyl oleate and methyl linoleate behind reflected shock waves, Proc. Combust. Inst. 34 (2013) 419–425.
[14] W. Wang, S. Gowdagiri, M.A. Oehlschlaeger, The high-temperature autoignition of biodiesels and biodiesel components, Combust. Flame. 161 (2014) 3014–3021.
[15] D.D. Das, C.S. McEnally, L.D. Pfefferle, Sooting tendencies of unsaturated esters in nonpremixed flames, Combust. Flame. 162 (2015) 1489–1497.
[16] M.F. Campbell, D.F. Davidson, R.K. Hanson, Ignition delay times of very-low-vapor-pressure biodiesel surrogates behind reflected shock waves, Fuel. 126 (2014) 271–281.
[17] C.T. Chong, S. Hochgreb, Measurements of laminar flame speeds of liquid fuels: Jet-A1, diesel, palm methyl esters and blends using particle imaging velocimetry (PIV), Proc. Combust. Inst. 33 (2011) 979–986.
[18] P. Dagaut, S. Gaïl, M. Sahasrabudhe, Rapeseed oil methyl ester oxidation over extended ranges of pressure, temperature, and equivalence ratio: Experimental and modeling kinetic study, Proc. Combust. Inst. 31 (2007) 2955–2961.
[19] M.H. Hakka, P.-A. Glaude, O. Herbinet, F. Battin-Leclerc, Experimental study of the oxidation of large surrogates for diesel and biodiesel fuels, Combust. Flame. 156 (2009) 2129–2144.
[20] S. Bax, M.H. Hakka, P.-A. Glaude, O. Herbinet, F. Battin-Leclerc, Experimental study of the oxidation of methyl oleate in a jet-stirred reactor, Combust. Flame. 157 (2010) 1220–1229.
[21] F. Battin-Leclerc, A. Rodriguez, B. Husson, O. Herbinet, P.-A. Glaude, Z. Wang, et al., Products from the Oxidation of Linear Isomers of Hexene, J. Phys. Chem. A. 118 (2014) 673–683.
[22] J. Biet, M.H. Hakka, V. Warth, P.-A. Glaude, F. Battin-Leclerc, Experimental and modeling study of the low-temperature oxidation of large alkanes, Energy Fuels. 22 (2008) 2258–2269.
[23] O. Herbinet, J. Biet, M.H. Hakka, V. Warth, P.-A. Glaude, A. Nicolle, et al., Modeling study of the low-temperature oxidation of large methyl esters from C11 to C19, Proc. Combust. Inst. 33 (2011) 391–398.
[24] C.V. Naik, C.K. Westbrook, O. Herbinet, W.J. Pitz, M. Mehl, Detailed chemical kinetic reaction mechanism for biodiesel components methyl stearate and methyl oleate, Proc. Combust. Inst. 33 (2011) 383–389.
[25] E. Ranzi, M. Dente, A. Goldaniga, G. Bozzano, T. Faravelli, Lumping procedures in detailed kinetic modeling of gasification, pyrolysis, partial oxidation and combustion of hydrocarbon mixtures, Prog. Energy Combust. Sci. 27 (2001) 99–139.
[26] C. Saggese, A. Frassoldati, A. Cuoci, T. Faravelli, E. Ranzi, A lumped approach to the kinetic modeling of pyrolysis and combustion of biodiesel fuels, Proc. Combust. Inst. 34 (2013) 427–434.

[27] O. Herbinet, B. Husson, M. Ferrari, P.-A. Glaude, F. Battin-Leclerc, Low temperature oxidation of benzene and toluene in mixture with n-decane, Proc. Combust. Inst. 34 (2013) 297–305.
[28] D. Ray, Waddingt.dj, Gas-Phase Oxidation of Alkenes .2. Oxidation of 2-Methylbutene-2 and 2,3-Dimethylbutene-2, Combust. Flame. 20 (1973) 327–334.
[29] D. Ray, A. Redfearn, Waddingt.dj, Gas-Phase Oxidation of Alkenes - Decomposition of Hydroxy-Substituted Peroxyl Radicals, J. Chem. Soc.-Perkin Trans. 2. (1973) 540–543.
[30] O. Herbinet, G. Dayma, Jet-Stirred Reactors, in: F. Battin-Leclerc, J.M. Simmie, E. Blurock (Eds.), Cleaner Combustion, Springer London, 2013: pp. 183–210.
[31] WebBook de Chimie NIST, NIST Chem. WebBook. (2015). http://webbook.nist.gov/chemistry/.
[32] P. Azay, G.-M. Côme, Temperature Gradients in a Continuous Flow Stirred Tank Reactor, Ind. Eng. Chem. Process Des. Dev. 18 (1979) 754–756.
[33] A. Andreatch, R. Feinland, Continuous Trace Hydrocarbon Analysis by Flame Ionization, Anal. Chem. 32 (1960) 1021–1024.
[34] W. Dietz, Response Factors for Gas Chromatographic Analyses, J. Gas Chromatogr. 5 (1967) 68–71.
[35] C.K. Westbrook, W.J. Pitz, M. Mehl, P.-A. Glaude, O. Herbinet, S. Bax, et al., Experimental and Kinetic Modeling Study of 2-Methyl-2-Butene: Allylic Hydrocarbon Kinetics, J. Phys. Chem. A. 119 (2015) 7462–7480.
[36] A. Cuoci, A. Frassoldati, T. Faravelli, E. Ranzi, OpenSMOKE++: An object-oriented framework for the numerical modeling of reactive systems with detailed kinetic mechanisms, Comput. Phys. Commun. 192 (2015) 237–264.
[37] R. Grana, A. Frassoldati, C. Saggese, T. Faravelli, E. Ranzi, A wide range kinetic modeling study of pyrolysis and oxidation of methyl butanoate and methyl decanoate – Note II: Lumped kinetic model of decomposition and combustion of methyl esters up to methyl decanoate, Combust. Flame. 159 (2012) 2280–2294.
[38] E. Ranzi, A. Frassoldati, S. Granata, T. Faravelli, Wide-Range Kinetic Modeling Study of the Pyrolysis, Partial Oxidation, and Combustion of Heavy n-Alkanes, Ind. Eng. Chem. Res. 44 (2005) 5170–5183.
[39] K.M. Van Geem, M.F. Reyniers, G.B. Marin, Challenges of Modeling Steam Cracking of Heavy Feedstocks, Oil Gas Sci. Technol. - Rev. IFP. 63 (2008) 79–94.
[40] R. Bounaceur, V. Warth, B. Sirjean, P.A. Glaude, R. Fournet, F. Battin-Leclerc, Influence of the position of the double bond on the autoignition of linear alkenes at low temperature, Proc. Combust. Inst. 32 (2009) 387–394.
[41] C.K. Westbrook, W.J. Pitz, S.M. Sarathy, M. Mehl, Detailed chemical kinetic modeling of the effects of C=C double bonds on the ignition of biodiesel fuels, Proc. Combust. Inst. 34 (2013) 3049–3056.
[42] C. Saggese, A. Frassoldati, A. Cuoci, T. Faravelli, E. Ranzi, A wide range kinetic modeling study of pyrolysis and oxidation of benzene, Combust. Flame. 160 (2013) 1168–1190.
[43] M.S. Stark, D.J. Waddington, Oxidation of propene in the gas phase, Int. J. Chem. Kinet. 27 (1995) 123–151.
[44] M. Mehl, G. Vanhove, W.J. Pitz, E. Ranzi, Oxidation and combustion of the n-hexene isomers: A wide range kinetic modeling study, Combust. Flame. 155 (2008) 756–772.
[45] H. Sun, J.W. Bozzelli, C.K. Law, Thermochemical and Kinetic Analysis on the Reactions of O2 with Products from OH Addition to Isobutene, 2-Hydroxy-1,1-dimethylethyl, and 2-Hydroxy-2-methylpropyl Radicals: HO2 Formation from Oxidation of Neopentane, Part II, J. Phys. Chem. A. 111 (2007) 4974–4986.
[46] C. Muller, V. Michel, G. Scacchi, G.M. Côme, THERGAS: a computer program for the evaluation of thermochemical data of molecules and free radicals in the gas phase, J. Chim. Phys. Phys.-Chim. Biol. 92 (1995) 1154–1178.

[47] S.W. Benson, Thermochemical Kinetics: Methods for the Estimation of Thermochemical Data and Rate Parameters, Edition: 2nd edition, John Wiley & Sons Inc, New York, 1976.
[48] E. Domalski, E. Hearing, Estimation of the Thermodynamic Properties of C-H-N-O-S-Halogen Compounds at 298.15-K, J. Phys. Chem. Ref. Data. 23 (1994) 157–159.
[49] W. Tsang, J.A. Walker, Pyrolysis of 1,7-octadiene and the kinetic and thermodynamic stability of allyl and 4-pentenyl radicals, J. Phys. Chem. 96 (1992) 8378–8384.
[50] M. Dente, Personal Communication, Personal Communication, (2015).
[51] W. Wang, M.A. Oehlschlaeger, A shock tube study of methyl decanoate autoignition at elevated pressures, Combust. Flame. 159 (2012) 476–481.
[52] C.K. Westbrook, Biofuels Combustion, Annu. Rev. Phys. Chem. 64 (2013) 201–219.